

Nonlinear dynamics of phase space zonal structures and energetic particle physics in fusion plasmas

F Zonca^{1,2}, L Chen^{2,3}, S Briguglio¹, G Fogaccia¹, G Vlad¹, X Wang⁴

¹ENEA C. R. Frascati, CP 65-00044 Frascati, Italy

²Institute for Fusion Theory and Simulation and Department of Physics, Zhejiang University, Hangzhou, 310027 P.R. China

³Department of Physics and Astronomy, University of California, Irvine CA 92697-4575, U.S.A.

⁴Max-Planck-Institut für Plasmaphysik, Boltzmannstr. 2, Garching D-85748, Germany

E-mail: fulvio.zonca@enea.it

Abstract. A general theoretical framework for investigating nonlinear dynamics of phase space zonal structures is presented in this work. It is then, more specifically, applied to the limit where the nonlinear evolution time scale is smaller or comparable to the wave-particle trapping period. In this limit, both theoretical and numerical simulation studies show that non-adiabatic frequency chirping and phase locking could lead to secular resonant particle transport on meso- or macro-scales. The interplay between mode structures and resonant particles then provides the crucial ingredient to properly understand and analyze the nonlinear dynamics of Alfvén wave instabilities excited by non-perturbative energetic particles in burning fusion plasmas. Analogies with autoresonance in nonlinear dynamics and with superradiance in free electron lasers are also briefly discussed.

PACS numbers: 52.35.Bj, 52.35.Mw, 52.55.Pi, 52.55.Tn, 52.35.Sb

Submitted to: *New J. Phys.*

1. Introduction

The important role of shear Alfvén waves (SAW) instabilities and their interaction with energetic particles/charged fusion products (EP) in burning fusion plasmas is widely acknowledged (cf., *e.g.*, [1, 2, 3]), and, historically, it was realized since the pioneering works by Belikov *et al* [4, 5], Rosenbluth and Rutherford [6] and Mikhailovskii [7, 8].

Alfvénic oscillations can be excited by EPs as well as thermal plasma components [9, 10], and, thus, are characterized by a broad spectrum of wavelengths, frequencies and growth rates, which are generally non-trivially interlinked due to the fact that short wavelength kinetic SAW can be excited by resonant mode conversion [11]. Therefore, these drift Alfvén waves (DAW) are expected to play important roles in complex behaviors of burning fusion plasmas [12, 13, 14, 15]; and may have the features of broad band turbulence with $\mathcal{O}(1)$ ratio between linear instability growth rate and mode frequency, $|\gamma_L/\omega_0| \sim 1$, or nearly periodic (quasi-coherent) nonlinear fluctuations with $|\gamma_L/\omega_0| \ll 1$ [1]. Meanwhile, such two components of the SAW/DAW spectrum have different effects on EP transports. In this work, the focus is on the nearly periodic (quasi-coherent) nonlinear fluctuations with $|\gamma_L/\omega_0| \ll 1$.

Alfvénic fluctuations in burning plasmas have typically low amplitudes, $\epsilon_\delta \equiv |\delta \mathbf{B}_\perp|/B_0 \lesssim 5 \times 10^{-4}$ [3], where the \perp subscript stands for perpendicular to the equilibrium magnetic field direction $\mathbf{b} \equiv \mathbf{B}_0/B_0$. Therefore, resonant EPs, more than non resonant ones, are expected to play crucial roles in transport processes [16, 17, 18, 19, 20]. Here, in particular, we consider transport processes in two-dimensional (2D) magnetized plasma equilibria with two periodic angle-like coordinates, (θ, ζ) , one of which (ζ) defines the equilibrium symmetry. Thus, phase space structures that are of direct interest are those obtained by averaging out dependences on angle-like variables. In fact, in the general procedure used for deriving kinetic equations in weakly-nonideal systems [21, 22, 23], these structures are those dominating the “principal series” of secular terms obtained by formal perturbation expansion in powers of fluctuating fields; which can be summed up and yields the solution of the corresponding Dyson equation [24, 25]. These phase space structures may be generally referred to as “phase space zonal structures” [15, 26, 27] (PSZS), by analogy with the meso-scale configuration space patterns spontaneously generated by drift-wave turbulence (DWT); *i.e.*, zonal flows and currents/fields or, more generally, zonal structures (ZS) [28, 29, 30, 31]. Here and in the following, meso-scales are intermediate length scales between the SAW/DAW/DWT micro-scales, typically ordered as the perpendicular fluctuation wavelength, λ_\perp , and the system-size macro-scales, characteristic of equilibrium plasma profiles and macroscopic fluctuations. In magnetized fusion plasmas, at the leading order, ZS are independent of (θ, ζ) ; due to finite magnetic shear, which suppresses convective cells [32, 33]. Hence, ZS do not significantly contribute to cross-field transport [34].

Both ZS and PSZS in fusion plasmas are transverse fluctuations, since they have $\mathbf{k} \cdot \mathbf{b} = 0$ everywhere, with \mathbf{k} the wave vector. Meanwhile, they describe the corrugations of equilibrium radial profiles [35, 36, 37] as consequence of fluctuation induced transport

processes, due to emission and reabsorption of (toroidal equilibrium) symmetry breaking perturbations [15]. In general, the time scale of ZS and PSZS evolution is the same as that of the underlying fluctuations, with important consequences on the meso-scale dynamics of SAW/DAW and DWT, which may become nonlocal and be characterized, *e.g.*, by avalanches [38, 39, 40, 41]. For understanding and explaining different behaviors of PSZS, it is important to compare the wave-particle trapping time, τ_B , with the characteristic time of nonlinear evolution of PSZS, τ_{NL} . When $\tau_B \ll \tau_{NL}$, there exists an adiabatic (action) invariant; and phase space density is preserved inside the structure separatrix. When this occurs, phase space holes and clumps [42, 43, 44, 45, 46, 47, 48] are limiting cases of PSZS, and the nonlinear evolution is referred to as “adiabatic”. Meanwhile, when $\tau_B \sim \tau_{NL}$, no adiabatic (action) invariant exists in the phase space, resonant particle motion can be secular, and the dynamics is “non-adiabatic”. Thus, different nonlinear behavior and EP transport are expected, in general, depending on the relative ordering of τ_B and τ_{NL} . This also suggests that qualitative and quantitative differences may be expected depending on whether fluctuations are externally controlled, such as in a “driven” system, or are resulting as consequence of plasma instabilities. In fact, while, in the former case, phase space dynamics is typically adiabatic; the evolution, in the instability case, often becomes non-adiabatic such that, at saturation, $\tau_{NL} \gtrsim \gamma_L^{-1}$ and $\tau_B \gtrsim \gamma_L^{-1}$ [27].

In this work, we analyze the case of nonlinear EP distribution functions that dynamically evolve on characteristic “transport” time scales, which are generally of the same order of the nonlinear time scale of the underlying instabilities [27, 35, 36]; *i.e.*, typically in the non-adiabatic regime. Furthermore, we assume that resonant wave-particle interaction between EPs and Alfvénic fluctuations in burning plasmas is non-perturbative; that is, EPs play significant roles in determining mode frequency and mode structure. Non-perturbative EP response to SAW/DAW instabilities is the crucial element characterizing PSZS nonlinear dynamics discussed in this work. By addressing the general non-adiabatic case, $\tau_{NL} \sim \gamma_L^{-1} \sim \tau_B$, the present approach can handle both the nonlinear saturation of EP driven Alfvénic instabilities, $\tau_{NL} \sim \gamma_L^{-1} \lesssim \tau_B$, as well as longer time scale nonlinear dynamics, $\tau_{NL} \gg \tau_B$, such as wave-particle trapping, quasi-linear diffusion, and collisional effects. The general theoretical framework is illustrated in Sec. 2, which demonstrates that “radial decoupling”, due to resonant EPs exploring finite radial structures of fluctuations in nonuniform plasmas, becomes increasingly more important than and eventually dominates “resonance detuning”, due to changing wave-particle phases. Such transition occurs when the size of nonlinear particle orbits is comparable with the radial fluctuation wavelength and corresponds to the onset of nonlocal behaviors; *i.e.*, of meso-scale dynamics. Mode frequency chirping and “phase locking” [16, 17, 26, 27, 35, 49, 50, 51, 52, 53] are shown to be the nonlinear dynamics by which secular resonant particle transport can occur on meso- and macro-scales. In order to illustrate theoretical framework and underlying concepts, Sec. 2 focuses on the obtained results and physics implications, while detailed analytical derivations are given in Appendix A. Furthermore, analogies with “autoresonance” [54, 55] in nonlinear

systems are pointed out in order to illustrate similarities and differences in the behaviors of “driven” systems and unstable fusion plasmas in the presence of non-perturbative EP free energy sources.

This work aims at presenting fundamental aspects of PSZS nonlinear dynamics to a broad readership; and, thus, presents these issues from different perspectives. For this reason, after discussing the cornerstones of theoretical framework in Sec. 2, we adopt numerical simulations to give examples of how these physics manifest themselves in practice. Thus, meso-scale dynamics of radially localized Energetic Particle Modes (EPMs [56]) are illustrated in Sec. 3, which demonstrates non-perturbative EP behaviors, phase locking and non-adiabatic frequency chirping by numerical simulation results with the extended Hybrid MHD Gyrokinetic Code (XHMGC) [57, 58]. Section 4, meanwhile, provides specific derivations and discussions of PSZS nonlinear dynamics within the framework of nonlinear gyrokinetic theory [59, 60]. In Sec. 5, the PSZS evolution equations are specialized to the simple case of precessional resonance, for which the nonlinear dynamics is that of 1D non-autonomous nonuniform system. This case allows to derive the general form of the corresponding Dyson equation; and to illustrate the onset of nonlocal behaviors as novel feature in contrast to the case of a 1D uniform plasma. As application of the general theoretical framework of Sec. 5, Sec. 6 analyzes convective amplification of EPM wave packets as avalanches; soliton-like structures in active media, accompanied by secular EP transports on macro-scales. EPM avalanches can be taken as paradigmatic example of “radial decoupling” and non-perturbative EP behaviors. In fact, because of “phase locking”, wave-particle resonance is limited only by the finite radial mode structure. At the same time, non-perturbative EP response causes the mode structure to adapt to the modified EP source. Ultimately, the spatiotemporal structure of EPM avalanches is, thus, the self-consistent result of “radial decoupling” and non-perturbative EP response. In Sec. 6, as further evidence of general implications of these physics, analogies with “superradiance” [61] operation regime [62] in free electron lasers (FEL) are also discussed. Section 7 finally gives summarizing remarks and conclusions, while Appendix B and Appendix C are devoted to illustrating detailed expressions and technical derivations, and are proposed to interested readers only.

2. Theoretical framework

We consider an axisymmetric toroidal magnetized plasma, and use (r, θ, ζ) toroidal flux coordinates with straight magnetic fields lines. Here, r is a radial-like magnetic flux coordinate, ζ is the toroidal symmetry coordinate (cf. Sec. 1), \mathbf{B}_0 is represented as in Eq. (A.1), and the magnetic field line pitch $q \equiv \mathbf{b} \cdot \nabla \zeta / \mathbf{b} \cdot \nabla \theta = q(r)$ is a flux function, given in Eq. (A.2). Details about the adopted equilibrium representation and flux coordinates are given in Appendix A. Introducing $\beta = 8\pi P_0 / B_0^2$ as the ratio of kinetic to magnetic pressures, we consider sufficiently low- β plasma equilibria with $|\nabla_\perp| \gg |\nabla_\parallel|$, such that compressional Alfvén waves are suppressed and magnetic field

compression can be solved explicitly via perpendicular pressure balance

$$\nabla_{\perp} (B_0 \delta B_{\parallel} + 4\pi \delta P_{\perp}) \simeq 0 . \quad (1)$$

Thus, δB_{\parallel} can be eliminated from governing equations of SAW/DAW and DWT, which are then described in terms of two fluctuating scalar fields; *i.e.*, the scalar potential $\delta\phi$ and the parallel (to \mathbf{b}) vector potential δA_{\parallel} . As usual, subscript 0 denotes equilibrium quantities and δ is the prefix of fluctuating fields.

As anticipated in Sec. 1, we assume that the characteristic nonlinear time, τ_{NL} , satisfies the following ordering [27, 63, 64]

$$1 \gg |\omega_0 \tau_{NL}|^{-1} \sim |\gamma_L / \omega_0| \gg \epsilon_{\omega} \equiv |\omega_0 / \Omega| , \quad (2)$$

with $\Omega = eB_0/(mc)$ the cyclotron frequency, which generally holds for SAW/DAW excited by EPs in fusion plasmas [15] but also applies to DWT in a variety of cases of practical interest [65, 66, 67, 68]. The ordering of Eq. (2) allows us to address the nonlinear saturation of the considered instabilities, as well as to investigate post-saturation dynamics.

2.1. Onset of nonlocal behaviors: resonance detuning and radial decoupling

Based on Eq. (2) and on the low SAW fluctuation amplitudes (cf. Sec. 1), it can be shown that resonant EP motion is slightly modified by fluctuations in one poloidal bounce/transit time. Therefore, fluctuation induced transport is a cumulative effect on resonant EP over many bounce/transit times, which can generally be secular, *i.e.*, not bounded in time. Detailed wave-particle interactions in axisymmetric toroidal magnetized plasmas are analyzed and discussed, under these assumptions, in Appendix A. There, it is shown that the effective action of a generic fluctuation field, $f(r, \theta, \zeta)$ (time dependences are left implicit), decomposed in Fourier harmonics, can be represented as

$$\begin{aligned} f(r, \theta, \zeta) &= \sum_{m,n \in \mathbb{Z}} e^{in\zeta - im\theta} f_{m,n}(r) \\ &\rightarrow \sum_{m,n,\ell \in \mathbb{Z}} e^{i(n\bar{\omega}_d + \ell\omega_b)\tau + i\Theta_{m,n,\ell}} \mathcal{P}_{m,n,\ell} \circ f_{m,n}(\bar{r} + \Delta r) , \end{aligned} \quad (3)$$

where ω_b is the bounce/transit frequency for magnetically trapped/circulating particles and $\bar{\omega}_d$ is the toroidal precessional frequency, which are defined in Eqs. (A.5) and (A.11), respectively. Furthermore, τ is a time-like parameter that identifies the particle position along its integrable trajectory in the reference equilibrium, ℓ is the bounce harmonic, \bar{r} is the bounce averaged radial coordinate, defined in Eq. (A.6); and the projection operators $\mathcal{P}_{m,n,\ell}$ are defined by Eq. (A.14). Meanwhile, Δr and $\Theta_{m,n,\ell}$ are the nonlinear radial particle displacement and the nonlinear wave-particle phase shift, defined in Eqs. (A.25) and (A.31), respectively. Mathematically, Eq. (3) is a lifting of $f(r, \theta, \zeta)$ to the phase space, using the time-like parameter τ to map the effective action of $f(r, \theta, \zeta)$ as the particle moves along its integrable equilibrium trajectory, identified by its constants of motion. Thus, Eq. (3) reveals the dual nature of fluctuating fields in kinetic descriptions of collisionless plasmas: (i) the field observed in the laboratory frame, which enters in

the evolution equation of mode structures; and (ii) the field effectively experienced by the particle in the particle-moving frame, which enters in the description of wave-particle resonances (cf. Appendix A.1).

For $\Theta_{m,n,\ell} = 0$ and $\Delta r = 0$, a fluctuation $\propto \exp(-i\omega_0 t)$ readily yields wave-particle resonance condition in the form of Eqs. (A.16) and (A.17), respectively, for magnetically trapped and circulating particles. Meanwhile, in the presence of fluctuations, Eq. (3) accounts for the cumulative bounce/transit averaged fluctuation effects, discriminating between “resonance detuning”, $\propto \exp(i\Theta_{m,n,\ell})$, and “radial decoupling” $\propto \mathcal{P}_{m,n,\ell} \circ f_{m,n}(\bar{r} + \Delta r)$. These concepts, introduced theoretically in Ref. [27] and further discussed below and in Appendix A.2, are important for understanding and explaining nonlinear dynamics of SAW/DAW in nonuniform plasmas. In fact, based on the “universal description of a nonlinear resonance” [69] as non-autonomous system with one degree of freedom, which yields a one-dimensional (1D) nonlinear pendulum Hamiltonian also referred to as “standard Hamiltonian” [70], resonance detuning is a general common feature of wave-particle interactions. On the contrary, radial decoupling exists only in nonuniform plasmas; and becomes important when Δr is comparable with the perpendicular wavelength, λ_\perp , of perturbation structures $\propto \mathcal{P}_{m,n,\ell} \circ f_{m,n}$, which can be estimated as $\lambda_\perp \sim \epsilon_\Delta |nq'|^{-1}$, $\epsilon_\Delta < 1$ being a control parameter depending on the considered fluctuation and the nonuniform plasma equilibrium, characterizing the mode transverse scale length [27]. Introducing the “finite interaction length”, Δr_L , as the value of Δr at which wave-particle resonance is lost due to plasma nonuniformity, Eq. (3) shows that a quantitative and qualitative difference in nonlinear dynamics must be expected depending on the relative ordering of Δr_L and λ_\perp . It is possible to show that $\Delta r_L \sim 3|\gamma_L/\omega_0|\lambda_n^{-1}r$, with $\lambda_n = |nrq'|$ for circulating particles and $\lambda_n = 1$ for magnetically trapped particles (cf. Appendix A.3, where the corresponding “finite interaction time” is introduced as well). For $\Delta r_L \ll \lambda_\perp$, the plasma responds like a uniform system, and similarities can be drawn between EP-SAW interactions in burning plasmas of fusion interest and a 1D uniform beam-plasma system near marginality [71]. This limit offers obvious advantages of adopting a simple 1D system for complex dynamics studies [71, 72]. However, as demonstrated first in numerical studies of Ref. [73] and further illustrated by recent numerical works [49, 74], important differences and novel behaviors of EP-SAW interactions in nonuniform plasmas appear for $\Delta r_L \gtrsim \lambda_\perp$; *i.e.* (cf. Appendix A.3)

$$|\gamma_L/\omega_0| \gtrsim \frac{\lambda_n}{3|nrq'|} \epsilon_\Delta, \quad (4)$$

where $\epsilon_\Delta < 1$ controls the perpendicular fluctuation scale length. Note that Eq. (4) depends on the type of resonance as well as system geometry and nonuniformity through the control parameters λ_n and ϵ_Δ [26, 27]. These numerical simulation studies, illustrate the importance of mode structures in the nonlinear dynamics of SAW/DAW excited by EPs, consistent with Eq. (4) and theoretical predictions [75, 76]; and with recent experimental observations in DIII-D, interpreted and explained on the basis of dedicated numerical simulations [77]. Thus, Eq. (4) can be considered as a condition

for the onset of nonlocal behaviors in SAW/DAW interactions with EPs; and as indication that the system behaves as a truly 3D nonuniform plasma, despite one isolated resonance can still be described as non-autonomous system with one degree of freedom [15, 27]. A systematic investigation of these issues is given in Ref. [53], based on numerical simulation experiments analyzed with phase space diagnostics developed from Hamiltonian mapping techniques.

2.2. Phase locking and non-adiabatic phase space dynamics

Equation (4) suggests that onset of nonlocal behaviors and possibly novel features of SAW/DAW-EP interactions with respect to the beam-plasma system could emerge for sufficiently strong EP drive [35]. This poses an interesting issue on whether EP dynamics can be considered perturbatively. For example, the “bump-on-tail paradigm” [27, 51, 78] (cf. a recent review by Breizman and Sharapov [72]) considers perturbative EP response, which does not modify the thermal plasma dielectric behavior [71]. Thus, in this paradigm, nonlinear dynamics is dominated by wave particle trapping, whose frequency ω_B (cf. Appendix A.3) provides the shortest characteristic temporal scale, τ_{NL}^{-1} . Consequently, there then exists a conserved phase space action connected with wave particle trapping; and nonlinear evolution of EP driven AEs becomes that of phase space holes and clumps, defined as regions with, respectively, lack of density and excess of density w.r.t. the surrounding phase space. These physics have been extensively investigated since the pioneering work by Bernstein, Greene and Kruskal (BGK) [42]; and used for analyzing nonlinear behaviors of 1D uniform Vlasov plasmas [43, 44, 45, 46, 47, 48], including sources and collisional dissipation [71, 79, 80]. If the frequency of hole-clump pairs slowly evolves in time [81, 82, 83, 84, 85, 86], it happens adiabatically at a rate $|\dot{\omega}| \ll \omega_B^2$, set by balancing the rate of energy extraction of the moving holes/clumps in the phase space with the fixed background dissipation[‡]. EP transport in velocity space occurs in “buckets” [87], similar to “bucket” EP transport in real space introduced in Ref. [88]. However, unless diffusive transport process are considered due to many overlapping resonances, the EP transport in real space predicted by the “bump-on-tail paradigm” is implicitly local, since it assumes $\Delta r_L \ll \lambda_\perp$ (cf. Sec. 2.1). These transport processes are also similar to “autoresonance” [54, 55], by which a nonlinear pendulum can be driven to large amplitude, evolving in time to instantaneously match its frequency with that of an external drive with sufficiently slow downward frequency sweeping.

It was noted by Friedland *et al* [89] that spontaneous (“autoresonant”) nonlinear evolution of phase space structures becomes poorly controllable, when the underlying fluctuations are plasma instabilities rather than being imposed externally. In this respect, non-perturbative EP behaviors become particularly crucial for AEs; when the

[‡] Note that the original adiabatic theory of Ref. [84] has been recently extended in Refs. [85, 86], but still remains local in the sense discussed in Sec. 2.1 and hereafter. More detailed discussions of this point are given in Refs. [15, 27].

following condition

$$|\Delta\omega_{EP}| \ll |\Delta\omega_{SAW}| \quad (5)$$

is no longer satisfied [63, 64]. Here, $\Delta\omega_{EP}$ is the EP induced complex frequency shift of AEs; and $\Delta\omega_{SAW}$ is the frequency mismatch between AEs and the closest frequency of the SAW continuous spectrum computed at the peak AE amplitude. When Eq. (5) is progressively broken, AE mode structures are also increasingly affected by EP dynamic response; consistent with theoretical analyses [63, 64, 75, 76] and numerical simulation results [49, 73, 77, 90, 91] as well as experimental observations (cf., *e.g.*, Refs. [77, 92]). Meanwhile, EP response is always non-perturbative for EPMs [56], excited within the SAW continuous spectrum as discrete fluctuations at the frequency maximizing wave-EP power exchange above the threshold condition set by continuum damping [27, 63, 64, 93].

Clearly, for non-perturbative EP dynamics and significant transports over the domain where fluctuations are localized, the interplay between mode evolution and EP radial redistributions has crucial impact on nonlinear dynamics. Two factors are fundamental for the nonlinear mode evolution: (i) the nonlinear frequency shift determined by EP redistributions, consistent with mode dispersion relation; and (ii) the change in growth rate, taking into account mode structure distortions and EP transports. Both effects are constrained, self-consistently, by the mode dispersive properties. For a given nonlinear frequency shift, there always exists a group of resonant EPs, with given phase w.r.t. the wave, that satisfies

$$|\tau_{NL}\dot{\Theta}_{m,n,l}|, |\tau_{NL}^2\ddot{\Theta}_{m,n,l}| \ll 1 \quad ; \quad (6)$$

i.e., “phase locking”; as shown explicitly for, respectively, circulating and magnetically trapped particles by Eqs. (A.41) and (A.42) (cf. Appendix A.3). These are the resonant EPs that instantaneously maximize wave-particle power exchange [16, 17, 26, 27, 35, 51, 52, 53], as they minimize resonance detuning. At the same time, frequency chirping connected with this process is non-adiabatic $|\dot{\omega}| \lesssim \omega_B^2$, as demonstrated by Eqs. (A.37), (A.41) and (A.42). This means that, with non-perturbative EP response, phase locking is signature of non-adiabatic frequency chirping and non-local EP redistributions; and *vice versa* [27]. Phase locking further extends (but not indefinitely) the finite interaction length and the corresponding finite interaction time (cf. Sec. 2.1 and Appendix A.3) by a factor $\epsilon_{\dot{\omega}}^{-1} > 1$. Here, $\epsilon_{\dot{\omega}}$ is defined by Eq. (A.45) and depends on the mode dispersive properties. It denotes the effectiveness of phase locking; and, in general, $\epsilon_{\dot{\omega}} < 1$ requires the EP dynamics being non-perturbative. Adiabatic chirping ($|\dot{\omega}| \ll \omega_B^2$) or fixed frequency modes are characterized by $\epsilon_{\dot{\omega}} \simeq 1$. Taking into account the extended finite interaction length, Eq. (4) can be rewritten as

$$|\gamma_L/\omega_0| \gtrsim \frac{\lambda_n}{3|nrq'|} \epsilon_{\Delta} \epsilon_{\dot{\omega}} \quad . \quad (7)$$

Equation (7) indicates the growth rate threshold for radial mode structures to importantly affect nonlinear dynamics and the transition to non-local EP behaviors. Detailed analysis, would, in general, require a full 3D kinetic description including

realistic equilibrium geometry and nonuniformity [26, 27]. Assuming typical plasma parameters and the fact that generally $\epsilon_{\Delta}\epsilon_{\omega} \lesssim 10^{-1}$, Eq. (7) yields the estimates that $|\gamma_L/\omega_0| \gtrsim 10^{-3}$ for magnetically trapped particles, and $|\gamma_L/\omega_0| \gtrsim 10^{-2}$ for circulating particles [1, 26, 27, 35, 36].

The onset of non-local EP behaviors, above the threshold given by Eq. (7), corresponds to nonlinear meso-scale dynamics involving mode structures [35, 73, 94, 95, 96, 97]. We discuss these processes in Sec. 3 by numerical simulation experiments, constructed *ad hoc* to illustrate phase locking and non-adiabatic frequency chirping. However, depending on the considered plasma equilibrium and the corresponding fluctuation spectrum; and for increasing EP drive strength, phase locking and nonlinear meso-scale dynamics can extend to macro-scales. In this way, phase locked EPs could be secularly transported outward by the “mode particle pumping” mechanism, originally introduced for explaining EP loss due to “fishbone” fluctuations [16]. Meanwhile, self-consistent interplay between nonlinear mode dynamics and EP transports may give rise to EPM “avalanches”, by which EPM wave packets are convectively amplified as they propagate radially, until they are quenched by spatial nonuniformity (cf. Sec. 6 and Appendix A.3).

3. Nonlinear dynamics of localized EPMs

The important roles of plasma non-uniformities and finite radial mode structures for the nonlinear evolution of EP-driven SAW were first discussed by Briguglio *et al* [73], using hybrid MHD gyrokinetic numerical simulations [98] applied to the analysis of low- n toroidal AE (TAE) and EPM. Further insights into these physics were provided by hybrid MHD gyrokinetic simulations of nonlinear BAE dynamics [49]; employing high-resolution phase space numerical diagnostics techniques based on Hamiltonian mapping [99]. Similar results have also been illustrated by nonlinear gyrokinetic simulations [74].

In order to demonstrate non-perturbative EP behaviors and phase locking more clearly, Briguglio *et al* [53] have carried out a “numerical simulation experiment” with the XHMG code [57, 58], investigating the nonlinear dynamics of radially localized EPM near the TAE frequency gap. With the aim of controlling the EPM radial localization and inhibiting the onset of EPM convective amplifications (cf. Sec. 6) [35, 94, 96], Ref. [53] selected a sufficiently flat equilibrium q profile, $q(r) = 1.1 + 0.8(r/a)^2$. Adjacent toroidal frequency gaps in the SAW continuous spectrum were, thus, so far apart that nonlocal couplings were minimized, as shown in Fig. 1 (upper panels). For a tokamak equilibrium with major/minor radii ratio $R_0/a = 10$, Fig. 1 (upper panels) illustrates the $n = 2$ SAW continuous spectrum as thin black curve in the background of the intensity contour plots of an $n = 2$ EPM at different times: $\omega_A t = 1200$ (right before mode saturation), $\omega_A t = 1287$ (during saturation phase) and $\omega_A t = 1320$ (at the end of the EPM burst), with $\omega_A = v_A/R_0$ computed at the magnetic axis and v_A the Alfvén speed. The thermal plasma density,

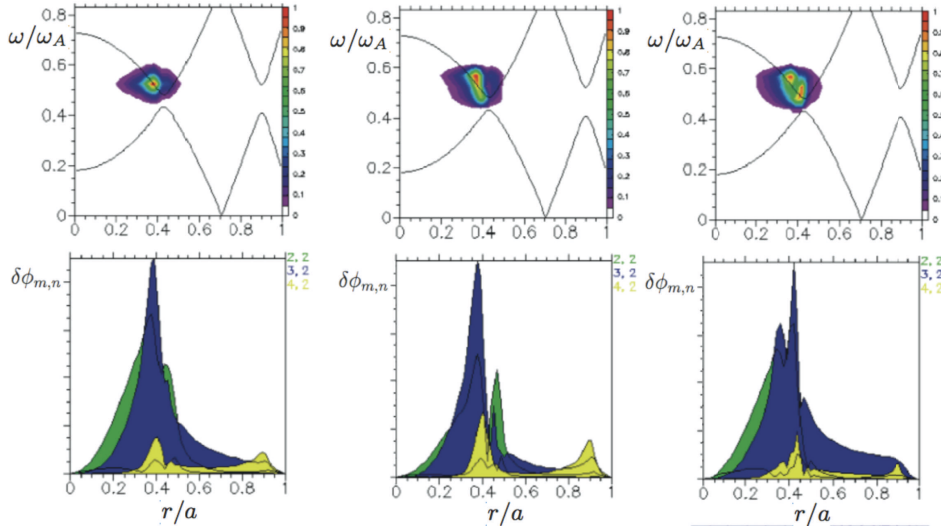


Figure 1. Three snapshots of the $n = 2$ EPM nonlinear evolution (adapted from the original Fig. 42 in Ref. [53]): $\omega_A t = 1200$ (left), $\omega_A t = 1287$ (middle) and $\omega_A t = 1320$ (right), with $\omega_A = v_A/R_0$ computed at the magnetic axis. The top panels are mode intensity contour plots in the $(r/a, \omega/\omega_A)$ plane, with the $n = 2$ SAW continuous spectrum shown by the thin black curve in background. Lower panels show the mode structures vs. r/a of individual EPM poloidal harmonics $\delta\phi_{m,n}$: $m = 2$ (green; 2nd dominant), $m = 3$ (blue; dominant) and $m = 4$ (yellow; subdominant). The $\delta\phi_{m,n}$ axis is normalized to the peak of the dominant harmonic. Reprinted with permission from Phys. Plasmas **21**, 112301 (2014). Copyright 2014, AIP Publishing LLC.

$n_i(r) = n_{i0}q^2(0)/q^2(r)$, is chosen such that the SAW frequency gaps are aligned, while the EP guiding-center distribution function (cf. Sec. 4) is a Maxwellian, $\bar{F}_{0EP} = (2\pi v_{EP})^{-3/2} n_E(r) \exp[-E/(m_{EP}v_{EP}^2)]$, with $n_{EP}(r) = n_{EP0} \exp[-\psi^2(r)/\psi^2(a)]$, $\psi(r)$ is the poloidal magnetic flux function introduced by Eq. (A.1), $n_{EP0}/n_{i0} = 1.75 \times 10^{-3}$, $v_{EP}/(a\Omega_{EP}) = 0.01$ and $v_{EP}/v_A = 1$ (cf. Ref. [53] for further numerical simulation details).

Kinetic Poincaré plots [53] in Fig. 2 show the dynamic evolution of EP PSZS for the same snapshots as in Fig. 1. Particle marker color denotes the initial P_ϕ , normalized to $m_{EP}v_{EP}a$, being larger (blue) or smaller (red) than the reference resonance value. The wave particle phase, Θ , meanwhile, is normalized to 2π and refers to $\Theta_{m,n,\ell}$ (cf. Sec. 2.1) computed for the dominant Fourier and bounce harmonics, $(m, n, \ell) = (3, 2, 1)$ [53], consistent with the transit resonance condition, Eq. (A.17). The P_ϕ axis is in a.u. and the Θ axis shows the range $0 \leq \Theta_{3,2,1} \leq 4\pi$ in order to better visualize EP PSZS. At $\omega_A t = 1200$ in Fig. 1(left), the mode is approaching saturation when EPs have completed $1/4$ oscillation in the instantaneous fluctuation-induced potential well, as confirmed by the corresponding kinetic Poincaré plot in Fig. 2; and the mode drive is significantly reduced at the original (linear) resonance location. In the further evolution of the mode and after mode saturation, the wave-particle power exchange becomes most negative (damping) at the original resonance location, when resonant EPs have completed $1/2$ oscillation in the instantaneous fluctuation-induced potential well, as shown in Fig. 2

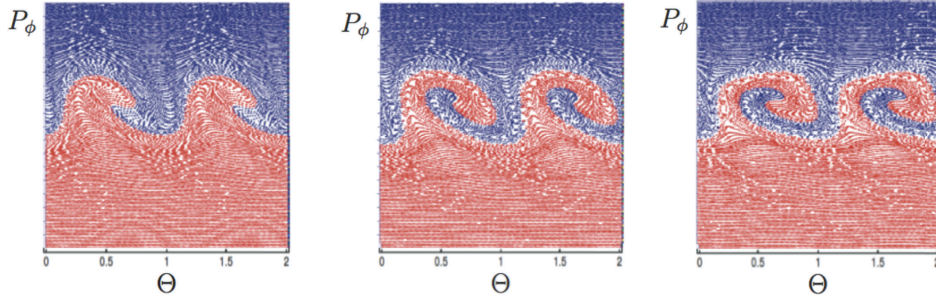


Figure 2. Kinetic Poincaré plots [53] illustrating the dynamic evolution of EP PSZS for the same snapshots as in Fig. 1. Normalization of phase space variables are discussed in the main text.

for $\omega_A t = 1287$. At the same time, due to the distortion of the EP distribution function, steeper gradient regions are formed at the outer limits of the PSZS, as these are the positions where particles tend to accumulate due to radial decoupling and diminishing fluctuation amplitude. This corresponds to an instantaneous strengthening of the mode drive at higher and lower frequencies, with respect to that of the original EPM (damped at this time), which “locally forces” wave-packets within the SAW continuous spectrum in the $(r/a, \omega/\omega_A)$ plane along the black lines in the background of the top panels of Fig. 1. Thus, the mode structure and frequency tend to split, as shown in both intensity contour plots and in mode structure plots of Fig. 1. Note that both mode saturation as well as mode structure and frequency splitting are non-adiabatic processes, since they occur on a time scale shorter than $2\pi\omega_B^{-1}$, as demonstrated in Fig. 2. Furthermore, phase locking plays an important role, since the radial dependence of SAW wave-packet frequency and of resonance condition, Eq. (A.17), is essentially the same; and, thus, Eq. (A.41), the phase locking condition, is readily satisfied. Consistent with the analysis of Sec. 2.2, non-adiabatic frequency chirping and phase locking are in one-to-one correspondence with non-perturbative EP behaviors. In fact, non-perturbative EP PSZS cause the two distinct dominant Fourier harmonics to shift radially and vary their relative weight; and yield the “rabbit-ear” structure of the $(3,2)$ mode, visible in the bottom right panel of Fig. 1, that would be otherwise not justifiable.

In the further nonlinear evolution, mode structure and frequency splitting become more evident in Fig. 1 for $\omega_A t = 1320$ (right), although the same features are still not visible in Fig. 2. As expected, mode structure splitting appears as double-resonance in the EP PSZS with some delay, as illustrated in Fig. 3 after $\simeq 3/4$ oscillation of resonant EP in the instantaneous fluctuation-induced potential well, due to the time required for EPs to effectively respond to the modified mode structures. After this phase, EP PSZS as well as corresponding mode structures and frequencies tend to merge again, yielding a second EPM burst [53]. As said above, this is due to the *ad hoc* setup of the present numerical simulation experiment, aimed at inhibiting the onset of EPM convective amplifications (cf. Sec. 6) [35, 94, 96]. Detailed investigations of these dynamics require an in depth discussion, which will be reported elsewhere. Here,

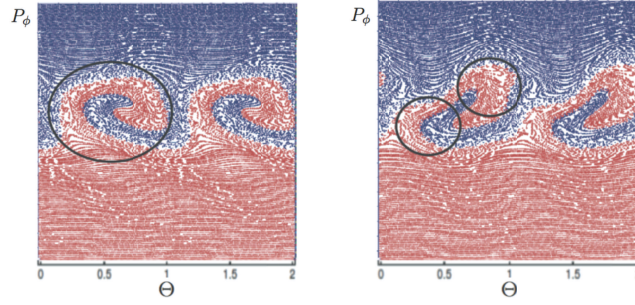


Figure 3. Kinetic Poincaré plots illustrating non-adiabatic transition from single (left, $\omega_A t = 1320$) to double (right, $\omega_A t = 1353$) resonance structures in the EP phase space. Time normalization is the same as in Fig. 1, while normalization of phase space variables are the same as in Fig. 2.

we emphasize again that both intensity contour plots and mode structure distortions are non-perturbative and evidently interlinked self-consistently with the non-adiabatic evolution of EP PSZS ($|\dot{\omega}| \sim \omega_B^2$). A crucial role is played by the “radial singular” structures characterizing the SAW continuous spectrum [15, 27, 63, 64]. In fact, while EP response to the regular EPM structure determines the mode frequency [56, 63, 64] and phase locking (cf. also Sec. 6), the mode structure is peaked (“singular”) at the radial position where the SAW continuous spectrum is resonantly excited. Thus, consistent with EP radial redistributions as they are transported nonlinearly, SAW wave-packets readily respond to instantaneous local forcing and maximize wave-particle power exchange. This is consistent with observations from numerical simulation results, reporting that SAW continuous spectrum is crucial in the nonlinear mode dynamics and frequency chirping [73, 94, 96, 97, 100, 101, 102, 103, 104] (cf. also Appendix A.3).

4. Governing equations of phase space zonal structures

As prevalent SAW/DAW and DWT fluctuations are in the low-frequency range, $|\omega_0| \ll |\Omega|$, kinetic description is based on the nonlinear gyrokinetic equation. Following Ref. [59], the perturbed particle distribution function δf can be written as

$$\delta f = e^{-\boldsymbol{\rho} \cdot \boldsymbol{\nabla}} \left[\delta g - \frac{e}{m} \frac{1}{B_0} \frac{\partial \bar{F}_0}{\partial \mu} \langle \delta L_g \rangle \right] + \frac{e}{m} \left[\frac{\partial \bar{F}_0}{\partial \mathcal{E}} \delta \phi + \frac{1}{B_0} \frac{\partial \bar{F}_0}{\partial \mu} \delta L \right]. \quad (8)$$

Here, adiabatic and non-adiabatic (δg) particle responses are separated, $e^{-\boldsymbol{\rho} \cdot \boldsymbol{\nabla}}$ is the *pull-back* transformation from guiding-center to particle coordinates [60], $\boldsymbol{\rho} \equiv \Omega^{-1} \mathbf{b} \times \mathbf{v}$, \bar{F}_0 is the equilibrium guiding-center particle distribution function,

$$\delta L_g = \delta \phi_g - \frac{v_{\parallel}}{c} \delta A_{\parallel g} = e^{\boldsymbol{\rho} \cdot \boldsymbol{\nabla}} \delta L = e^{\boldsymbol{\rho} \cdot \boldsymbol{\nabla}} \left(\delta \phi - \frac{v_{\parallel}}{c} \delta A_{\parallel} \right), \quad (9)$$

$\langle \dots \rangle$ denotes gyrophase averaging, $\mathcal{E} = v^2/2$ is the energy per unit mass, and μ is the magnetic moment adiabatic invariant (cf. Appendix A). Meanwhile, δg is obtained from the Frieman-Chen nonlinear gyrokinetic equation [59]

$$\left(\frac{\partial}{\partial t} + v_{\parallel} \nabla_{\parallel} + \mathbf{v}_d \cdot \boldsymbol{\nabla}_{\perp} + \delta \dot{\mathbf{X}}_{\perp} \cdot \boldsymbol{\nabla}_{\perp} \right) \delta g =$$

$$- \left(\frac{e}{m} \frac{\partial}{\partial t} \langle \delta L_g \rangle \frac{\partial \bar{F}_0}{\partial \mathcal{E}} + \frac{c}{B_0} \mathbf{b} \times \nabla \langle \delta L_g \rangle \cdot \nabla \bar{F}_0 \right), \quad (10)$$

where \mathbf{v}_d is the magnetic drift velocity

$$\mathbf{v}_d = \frac{\mathbf{b}}{\Omega} \times (\mu \nabla B_0 + \kappa v_{\parallel}^2) \simeq \frac{(\mu B_0 + v_{\parallel}^2)}{\Omega} \mathbf{b} \times \kappa, \quad (11)$$

$\kappa = \mathbf{b} \cdot \nabla \mathbf{b}$ is the magnetic field curvature and $\nabla B_0 \simeq \kappa B_0$ in the low- β limit. Furthermore, the fluctuation induced particle drift is

$$\delta \dot{\mathbf{X}}_{\perp} = \frac{c}{B_0} \mathbf{b} \times \nabla \langle \delta L_g \rangle + \frac{v_{\parallel}}{B_0} \kappa \langle \delta A_{\parallel g} \rangle = \frac{c}{B_0} \mathbf{b} \times \nabla \langle \delta \phi_g \rangle + v_{\parallel} \frac{\langle \delta \mathbf{B}_{\perp g} \rangle}{B_0}, \quad (12)$$

with $\langle \delta \mathbf{B}_{\perp g} \rangle = \nabla \times \mathbf{b} \langle \delta A_{\parallel g} \rangle$. Note that Eq. (8) is valid up to $\mathcal{O}(\epsilon_\delta)$ and that the relationship between δg and the fluctuating gyrocenter distribution function $\delta \bar{F}$ is given by $\delta \bar{F} = \delta g + (e/m) \partial_{\mathcal{E}} \bar{F}_0 \langle \delta L_g \rangle$ [60]. This approximation is justified within the characteristic (linear/nonlinear) time scale ordering of Eq. (2) (cf. Appendix A.2 for further discussions).

Consistent with Sec. 1, the “principal series” of secular terms obtained by formal perturbation expansion in powers of fluctuating fields is dominated by PSZS [21, 22, 23], which can be summed up and yields the solution of the corresponding Dyson equation [24, 25] (cf. Sec. 5). Thus, we formally separate $(m, n, \ell) = (0, 0, 0)$ terms in Eq. (3) from $n \neq 0$ responses. PSZS, denoted hereafter by the subscript z , are then described by the distribution function δf_z , decomposed according to Eq. (8); *i.e.*,

$$\begin{aligned} \delta f_z = & \sum_m \left\{ \mathcal{P}_{m,0,0} \circ [J_0(\lambda) \delta g]_{m,0} \right\} - \left[J_0(\lambda) \left(\frac{e}{m} \frac{1}{B_0} \frac{\partial \bar{F}_0}{\partial \mu} \langle \delta L_g \rangle \right) \right]_{0,0} \\ & + \frac{e}{m} \left[\frac{\partial \bar{F}_0}{\partial \mathcal{E}} \delta \phi + \frac{1}{B_0} \frac{\partial \bar{F}_0}{\partial \mu} \delta L \right]_{0,0}. \end{aligned} \quad (13)$$

Here, the double subscript on fields stands for (m, n) , $J_0(\lambda) = \langle e^{\rho \cdot \nabla} \rangle$ accounts for finite Larmor radius effects and $\lambda = k_{\perp} v_{\perp} / \Omega$. Assuming $|k_{\parallel}| \ll |\mathbf{k}_{\perp}|$, the PSZS non-adiabatic response can be derived from Eqs. (3) and (10); and is given by [27, 35]

$$\begin{aligned} \frac{\partial \delta g_z}{\partial t} = & - \mathcal{P}_{0,0,0} \circ \left(\frac{e}{m} \frac{\partial}{\partial t} \langle \delta L_g \rangle_z \frac{\partial \bar{F}_0}{\partial \mathcal{E}} \right)_{0,0} \\ & + i \sum_m \mathcal{P}_{m,0,0} \circ \frac{c}{d\psi/dr} \frac{\partial}{\partial r} \sum_{n \neq 0} n (\delta g_n \langle \delta L_g \rangle_{-n})_{m,0}, \end{aligned} \quad (14)$$

where ψ is the poloidal magnetic flux, \mathbf{B}_0 is represented as in Eq. (A.1), while the first and second terms on the right hand side (RHS) represent, respectively, the effects of ZS (zonal flows/fields) and the corrugation of radial profiles. Note that the formally nonlinear terms $\propto n$ on the RHS are dominant for $n \neq 0$ and $|k_{\parallel}| \ll |\mathbf{k}_{\perp}|$ modes, consistent with the standard gyrokinetic equation orderings [59, 60]. However, if the nonlinear interactions between PSZS and ZS themselves are considered, Eq. (14) should be suitably modified and an additional nonlinear term should be added on the RHS (cf. Refs. [51, 105]). This is beyond the scope of the present paper, focusing on the

nonlinear interaction of PSZS with $n \neq 0$ SAW/DAW; and is reported here only for the sake of completeness.

Following the same procedure, the evolution equation for δg_n can be derived from Eqs. (3) and (10), yielding

$$\begin{aligned} \left(\frac{\partial}{\partial t} - \frac{inc}{d\psi/dr} \frac{\partial \langle \delta L_g \rangle_z}{\partial r} + v_{\parallel} \nabla_{\parallel} + \mathbf{v}_d \cdot \nabla_{\perp} \right) \delta g_n = \\ = i \frac{e}{m} \left(Q \bar{F}_0 - \frac{n B_0}{\Omega d\psi/dr} \frac{\partial}{\partial r} \mathcal{P}_{0,0,0} \circ \delta g_z \right) \langle \delta L_g \rangle_n . \end{aligned} \quad (15)$$

$$Q \bar{F}_0 = \frac{\partial \bar{F}_0}{\partial \mathcal{E}} i \frac{\partial}{\partial t} + \frac{\mathbf{b} \times \nabla \bar{F}_0}{\Omega} \cdot (-i \nabla) . \quad (16)$$

On the left hand side (LHS) of Eq. (15), it is interesting to note the effect of ZS in enhancing resonance detuning. Meanwhile, on the RHS, PSZS modify the mode dynamics via corrugation of resonant particle radial profiles. The lack of symmetry between effects of spatial and velocity space gradients of PSZS is only due to having dropped the $\propto \delta \dot{\mathcal{E}} \partial_{\mathcal{E}} \delta g_n$ term on the LHS of Eq. (10), with

$$\delta \dot{\mathcal{E}} = -\frac{e}{m} \mathbf{v}_d \cdot \nabla_{\perp} \langle \delta L_g \rangle , \quad (17)$$

consistent with the standard gyrokinetic equation orderings [59, 60]. Similar to Eq. (14), this term must be restored when considering nonlinear interactions between PSZS and ZS themselves [51, 105].

Noting Eq. (A.18), fluctuation induced radial and energy excursion are ordered as $\Delta r/r \sim (\omega_{*EP}/\omega_0) \Delta \mathcal{E}/\mathcal{E}$ [27, 106], with ω_{*EP} the EP diamagnetic frequency and $|\omega_{*EP}/\omega_0| \gg 1$ for EP driven SAW/DAW in fusion plasmas (cf. Appendix A.3). Taking into account the definition of the $Q \bar{F}_0$ operator in Eq. (16), Eq. (15) can then be rewritten as

$$\left(\frac{\partial}{\partial t} - \frac{inc}{d\psi/dr} \frac{\partial \langle \delta L_g \rangle_z}{\partial r} + v_{\parallel} \nabla_{\parallel} + \mathbf{v}_d \cdot \nabla_{\perp} \right) \delta g_n = -\frac{inc}{d\psi/dr} \frac{\partial F_0}{\partial r} \langle \delta L_g \rangle_n . \quad (18)$$

Here, we have introduced

$$F_0 \equiv \bar{F}_0 + \mathcal{P}_{0,0,0} \circ \delta g_z ; \quad (19)$$

and have consistently neglected $\mathcal{O}(\omega_0/\omega_{*EP})$ terms on the RHS [27]. Using Eq. (19), Eq. (14) can be cast as

$$\begin{aligned} \frac{\partial F_0}{\partial t} = & -\mathcal{P}_{0,0,0}^2 \circ \left(\frac{e}{m} \frac{\partial}{\partial t} \langle \delta L_g \rangle_z \frac{\partial \bar{F}_0}{\partial \mathcal{E}} \right)_{0,0} \\ & + i \mathcal{P}_{0,0,0} \circ \sum_m \mathcal{P}_{m,0,0} \circ \frac{c}{d\psi/dr} \frac{\partial}{\partial r} \sum_{n \neq 0} n (\delta g_n \langle \delta L_g \rangle_{-n})_{m,0} . \end{aligned} \quad (20)$$

On the RHS, the dominant contribution in the nonlinear dynamics of EP PSZS is fluctuation induced resonant particle scattering. In Eq. (20), however, the contribution of other collisional [71] and non-collisional [107, 108, 109, 110] scattering processes may be readily included by corresponding scattering operators. Collision induced

scattering, introduced in Ref. [71], was the first one to be considered; but micro-turbulence induced diffusion has been demonstrated to be more relevant in typical ITER conditions [109, 110]. Radio-frequency wave induced scattering [107] has also been shown to dominate over collisional scattering in conditions of practical interest in present day experiments [108]. These additional physics affect the nonlinear evolution of F_{0EP} via self-consistent interplay of SAW/DAW and non-perturbative EP responses on typical time scales longer than those considered here, $\tau_{NL} \sim \gamma_L^{-1}$; and, thus, will be neglected.

Equations (18) and (20) completely describe PSZS nonlinear dynamics, once they are closed by evolution equations for SAW/DAW, $\langle \delta L_g \rangle_n$, and ZS, $\langle \delta L_g \rangle_z$. They also suggest that nonlinear dynamics of ZS and PSZS may be viewed as generators of neighboring nonlinear equilibria, which generally vary on the same time scale of the underlying fluctuation spectrum [37]. Here, leaving time dependences implicit and using the Poisson summation formula, we follow Ref. [111] and write the spatiotemporal structures of SAW/DAW as [15]

$$\begin{aligned} \delta\phi_n(r, \theta, \zeta) &= 2\pi \sum_{\ell \in \mathbb{Z}} e^{in\zeta - inq(\theta - 2\pi\ell)} \hat{\delta\phi}_n(r, \theta - 2\pi\ell) \\ &= \sum_{m \in \mathbb{Z}} e^{in\zeta - im\theta} \int e^{i(m-nq)\vartheta} \hat{\delta\phi}_n(r, \vartheta) d\vartheta, \end{aligned} \quad (21)$$

with the same decomposition assumed for $\delta A_{\parallel n}$. Meanwhile, separating parallel mode structure, $\delta\hat{\phi}_{0n}$, and radial envelope, $A_n(r)$, we let [15]

$$\delta\hat{\phi}_n(r, \vartheta) = A_n(r) \delta\hat{\phi}_{0n}(r, \vartheta). \quad (22)$$

Finally, we adopt the theoretical framework of the general fishbone like dispersion relation (GFLDR) [63, 64], that allows to write SAW/DAW dynamics equations as

$$[i\Lambda_n - (\delta\bar{W}_f + \delta\bar{W}_k)_n] A_n(r) = D_n(r, \theta_k, \omega) A_n(r) = 0, \quad (23)$$

which should be intended as the n -th row of a matrix equation for the complex amplitudes (\dots, A_n, \dots) involving nonlinear mode couplings [27, 36]. Equation (23) is obtained by projection of nonlinear gyrokinetic quasineutrality condition and vorticity equation on the parallel mode structures $\delta\hat{\phi}_{0n}(r, \vartheta)$; and assumes the eikonal form $A_n(r) \sim \exp i \int nq' \theta_k(r) dr$ [112, 113]. Thus, $D_n(r, \theta_k, \omega)$ plays the role of a local WKB nonlinear dispersion function, but it can also be written for global fluctuations [63, 64]. General expressions of Λ_n , $\delta\bar{W}_{fn}$ and $\delta\bar{W}_{kn}$ are derived in Refs. [63, 64] and given in Appendix B without derivation for readers' convenience: Λ_n represents a generalized “inertia” accounting for the structures of the SAW continuous spectrum; while $\delta\bar{W}_{fn}$ and $\delta\bar{W}_{kn}$ can be interpreted as fluid and kinetic “potential energies” [17]. Adopting the time scale ordering of Eq. (2), the spatiotemporal evolution of SAW wave packets can be described expanding the solutions of Eq. (23) about the linear characteristics

$$D_n^L(r, \theta_{k0}(r), \omega_0) = 0, \quad (24)$$

where D_n^L is the linearized dispersion function introduced in Eq. (23). Thus, letting $A_n(r) = \exp(-i\omega_0 t) A_{n0}(r, t)$, the spatiotemporal evolution equation for $A_{n0}(r, t)$

becomes [63, 111]

$$\begin{aligned} \frac{\partial D_n^L}{\partial \omega_0} \left(i \frac{\partial}{\partial t} \right) A_{n0} + \frac{\partial D_n^L}{\partial \theta_{k0}} \left(-\frac{i}{nq'} \frac{\partial}{\partial r} - \theta_{k0} \right) A_{n0} + \frac{1}{2} \frac{\partial^2 D_n^L}{\partial \theta_{k0}^2} \\ \times \left[\left(-\frac{i}{nq'} \frac{\partial}{\partial r} - \theta_{k0} \right)^2 A_{n0} - \frac{i}{nq'} \frac{\partial \theta_{k0}}{\partial r} A_{n0} \right] = S_n(r, t) . \end{aligned} \quad (25)$$

The $S_n(r, t)$ term on the RHS represents a generic source term, including external forcing, $S_n^{\text{ext}}(r, t)$, and/or nonlinear interactions, denoted by the superscript NL and extracted from the definition of D_n in Eq. (23) [27, 63, 111]

$$S_n(r, t) = S_n^{\text{ext}}(r, t) - e^{i\omega_0 t} \left[i\Lambda_n^{NL} - (\delta\bar{W}_f^{NL} + \delta\bar{W}_k^{NL})_n \right] e^{-i\omega_0 t} A_{n0} . \quad (26)$$

Equation (25) also holds as evolution equation for global modes, provided that A_{n0} is interpreted as mode amplitude at a fixed radial position and D_n is suitably redefined as a global dispersion function operator [63], with $\partial_r D_n = \partial_{\theta_k} D_n = \partial_{\theta_k}^2 D_n = 0$. By letting $A_{n0}(r, t) \rightarrow A_z(r, t) \equiv e^{i\omega_z t} \delta\phi_z$, with ω_z the ZS complex frequency, Eq. (25) also describes zonal flow dynamics, while the zonal field evolution, assuming massless fluid electron response, is given by [27]

$$\frac{\partial}{\partial t} \delta A_{\parallel z} = \left(\frac{c}{B_0} \mathbf{b} \times \nabla \delta A_{\parallel} \cdot \nabla \delta \psi \right)_z , \quad (27)$$

with $\mathbf{b} \cdot \nabla \delta \psi \equiv -c^{-1} \partial_t \delta A_{\parallel}$ for $k_{\parallel} \neq 0$ modes.

In summary, Eqs. (18) and (20), closed by Eqs. (25) and (27), describe the self-consistent evolution of ZS and PSZS in the presence of SAW/DAW and/or DWT, based on the time scale ordering of Eq. (2). Despite their relatively simple form, they have been investigated, so far, only in simplified limiting cases; *i.e.*, either neglecting the nonlinear effect of wave-particle resonances [37, 65, 66, 78, 114, 115, 116], or the effects of ZS [35, 36, 117, 118]. In particular, Eqs. (18) and (20) can describe the onset of nonlocal behaviors in SAW/DAW nonlinear dynamics and ensuing EP transport, discussed in Sec. 2.1; and the extension of secular EP transport from meso- to macro-scales due to phase locking, described in Sec. 2.2. It was noted in Sec. 2, that the onset of nonlocal behaviors is the signature that, even for an isolated resonance described as a 1D non-autonomous system, the nonuniform plasma dynamics is fully 3D. It is, however, particularly simple and instructive to investigate this problem for precessional resonance only; *i.e.*, Eq. (A.16) with $\ell = 0$. In such a case, in fact, assuming $\omega_0 \sim n\bar{\omega}_d \ll \omega_b$, EP nonlinear dynamics preserves both μ and J (cf. Appendix A). Thus, the problem is that of a 1D non-autonomous nonuniform system, which can be readily compared with the case of a 1D non-autonomous uniform plasma; *e.g.*, the “bump-on-tail paradigm” (cf. Sec. 2.2).

5. Dyson equation and the “fishbone paradigm”

In order to simplify the present analysis, we neglect ZS and restrict Eqs. (18) and (20) to precessional resonance with magnetically trapped EPs, while neglecting finite magnetic

drift orbit width effects and assuming $\omega_0 \sim n\bar{\omega}_d \ll \omega_b$. In this limit, as anticipated at the end of Sec. 4, we reduce the problem to analyzing a 1D non-autonomous nonuniform system, where onset of nonlocal behaviors is exclusively due to bounce averaged nonlinear EP dynamics. This is the simplest possible case of PSZS evolution, self-consistently interacting with SAW/DAW excited by EPs in fusion plasmas, and has been dubbed as “fishbone paradigm” [27, 51, 78]. In fact, this is also the case considered originally in the analysis of EP transport and nonlinear burst cycle of resonantly excited internal kink modes [16, 17], after their observation as “fishbone” oscillations in the Poloidal Divertor Experiment (PDX) [119]. The peculiar feature of the “fishbone paradigm”, emphasized in Refs. [27, 51, 78], is the self-consistent interplay of mode structures and EP transport, reflecting equilibrium geometry and plasma nonuniformity. In the following, we also show that the “fishbone paradigm” recovers the “bump-on-tail paradigm” in the (local) uniform plasma limit [27, 78].

5.1. Renormalization of phase space zonal structures

Noting Eq. (3), and due to the frequency ordering $\omega_0 \sim n\bar{\omega}_d \ll \omega_b$ as well as to the negligible magnetic drift orbit width limit, we can rewrite Eq. (20) in terms of

$$\delta\bar{\phi}_n = e^{in(\zeta-q\theta)} \sum_m \mathcal{P}_{m,n,0} \circ \delta\phi_{m,n} = e^{-inq\theta} \overline{e^{inq\theta} \delta\phi_n} , \quad (28)$$

with $\overline{(\dots)} = (2\pi)^{-1} \omega_b \oint (\dots) d\theta / \dot{\theta}$ denoting magnetic drift bounce averaging (cf. Appendix A); and the corresponding EP response

$$\delta\bar{g}_n = e^{in(\zeta-q\theta)} \sum_m \mathcal{P}_{m,n,0} \circ \delta g_{m,n} = e^{-inq\theta} \overline{e^{inq\theta} \delta g_n} . \quad (29)$$

Thus, recalling that the bounce averaged parallel velocity vanishes for magnetically trapped particles, we have

$$\begin{aligned} \frac{\partial F_0}{\partial t} &= i \sum_n \frac{nc}{d\psi/dr} \frac{\partial}{\partial r} (\delta\bar{g}_n \delta\bar{\phi}_{-n} - \delta\bar{g}_{-n} \delta\bar{\phi}_n) \\ &= \sum_n \frac{nc}{d\psi/dr} \frac{\partial}{\partial r} \left[\frac{nc}{d\psi/dr} \frac{\partial F_0}{\partial r} \frac{\partial}{\partial t} \left| \frac{\delta\bar{\phi}_n}{\omega_n} \right|^2 + i (\delta\bar{K}_n \delta\bar{\phi}_{-n} - \delta\bar{K}_{-n} \delta\bar{\phi}_n) \right] . \end{aligned} \quad (30)$$

Here, we have used the definition

$$\delta g \equiv \delta K + i(e/m) Q \bar{F}_0 \partial_t^{-1} \langle \delta\psi_g \rangle \quad (31)$$

and the ideal MHD condition $\delta E_{\parallel} = 0$; *i.e.*, $\delta\phi = \delta\psi$, defined below Eq. (27), to explicitly rewrite the RHS of Eq. (30), formally separating reversible from irreversible processes connected with wave-particle interactions, which dominate the nonlinear dynamics in Eq. (30). In fact, the contribution of reversible processes is $\mathcal{O}(\gamma_L \tau_{NL}^{-1} / \omega_0^2) \sim \mathcal{O}(\gamma_L^2 / \omega_0^2)$ with respect to irreversible ones, consistent with Eqs. (36) and (45) below. Hence, they will be neglected in the following. Adopting the notation

$$\hat{F}_0(\omega) = (2\pi)^{-1} \int_0^\infty e^{i\omega t} F_0(t) dt \quad (32)$$

for the Fourier-Laplace transform, Eq. (30) can be solved as

$$\begin{aligned} \hat{F}_0(\omega) = & \frac{i}{\omega} \text{St} \hat{F}_0(\omega) + \frac{i}{\omega} \hat{S}_0(\omega) + \frac{i}{2\pi\omega} \bar{F}_0(0) + \frac{nc}{\omega(d\psi/dr)} \\ & \times \frac{\partial}{\partial r} \int_{-\infty}^{\infty} \left[\delta \hat{\phi}_n(y) \delta \hat{K}_{-n}(\omega - y) - \delta \hat{\phi}_{-n}(y) \delta \hat{K}_n(\omega - y) \right] dy . \end{aligned} \quad (33)$$

Here, we have straightforwardly included the effect of collisions, formally denoted by $\text{St} \hat{F}_0(\omega)$, and of an external source term, $\hat{S}_0(\omega)$. Furthermore $\bar{F}_0(0)$ stands for the initial value of F_0 at $t = 0$, while the repeated n subscript assumes implicit summation. Note, also, that we have explicitly indicated only the dependences on ω (and y , as dummy integration frequency variable) for the sake of notation clarity. Meanwhile, for EP precessional resonance, it is possible to show [27]

$$\delta \hat{K}_n(\omega) = \frac{e}{m} \int_{-\infty}^{+\infty} \frac{\hat{\omega}_{dn}}{y} \frac{Q_{n,y} \hat{F}_0(\omega - y)}{n\bar{\omega}_d - \omega} \delta \hat{\phi}_n(y) dy , \quad (34)$$

where the subscripts in $Q_{n,y} \hat{F}_0$ denote mode number and frequency at which the operator defined by Eq. (16) must be evaluated; and, consistent with Eqs. (28) and (29), we have introduced the definition

$$e^{-inq\theta} \overline{e^{inq\theta} \omega_d \delta \phi_n} \equiv \hat{\omega}_{dn} \delta \hat{\phi}_n . \quad (35)$$

It is straightforward to verify that Eq. (34) gives back the linear limit for $\hat{F}_0(\omega) = (2\pi\omega)^{-1} i \bar{F}_0(0)$. By substitution of Eq. (34) into Eq. (33), one readily obtains

$$\begin{aligned} \hat{F}_0(\omega) = & \frac{i}{\omega} \text{St} \hat{F}_0(\omega) + \frac{i}{\omega} \hat{S}_0(\omega) + \frac{i}{2\pi\omega} \bar{F}_0(0) + \frac{e}{m} \frac{nc}{\omega(d\psi/dr)} \\ & \times \frac{\partial}{\partial r} \iint_{-\infty}^{\infty} \left[\delta \hat{\phi}_n(y) \frac{\hat{\omega}_{d-n}}{y'} \frac{Q_{-n,y'} \hat{F}_0(\omega - y - y')}{-n\bar{\omega}_d + y - \omega} \delta \hat{\phi}_{-n}(y') \right. \\ & \left. - \delta \hat{\phi}_{-n}(y) \frac{\hat{\omega}_{dn}}{y'} \frac{Q_{n,y'} \hat{F}_0(\omega - y - y')}{n\bar{\omega}_d + y - \omega} \delta \hat{\phi}_n(y') \right] dy dy' . \end{aligned} \quad (36)$$

This equation is the analogue of the Dyson equation in quantum field theory (cf., *e.g.*, Ref. [120]) describing EP transport due to emission and reabsorption of (toroidal equilibrium) symmetry breaking perturbations on all possible “loops” [15], schematically shown in Fig. 4. Its solution provides the renormalized expression of \hat{F}_0 , and, thereby, of F_0 , taking into account nonuniform toroidal plasmas effects with the addition of sources and collisions. The nonlinear term in Eq. (36) can be further simplified considering that

$$Q_{n,\omega} \hat{F}_0 \simeq - \frac{nB_0}{\Omega d\psi/dr} \frac{\partial \hat{F}_0}{\partial r} \quad (37)$$

for $|\omega_{*EP}/\omega| \gg 1$, typical of SAW/DAW excited by EP in fusion plasmas (cf. Sec. 4).

5.2. The uniform plasma limit and the bump-on-tail paradigm

The uniform plasma limit of Eq. (36) illuminates the connection of “fishbone” and “bump-on-tail” paradigms (cf. Secs. 2.2 and 4). It is obtained postulating constant

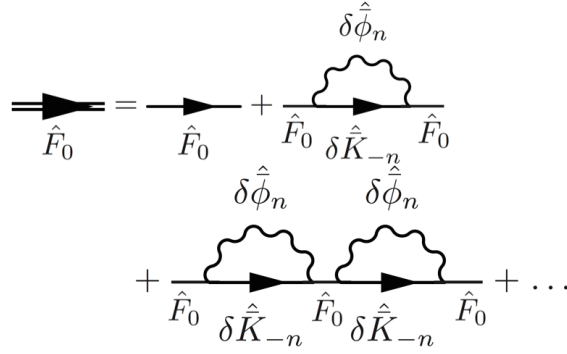


Figure 4. Schematic view of the Dyson series describing EP transport due to emission and reabsorption of (toroidal equilibrium) symmetry breaking perturbations [15].

$\delta\hat{\phi}_n(\omega)$ fluctuations and neglecting spatial dependences of \hat{F}_0 by mapping them into corresponding velocity space variations. By direct inspection of Eqs. (15) and (16), and by their comparison with the nonlinear Vlasov equation for a 1D uniform plasma, the configuration (radial) to velocity space mapping is obtained by letting

$$-\frac{nB_0}{d\psi/dr} \frac{\partial}{\partial r} \leftrightarrow k_0 \frac{\partial}{\partial v} . \quad (38)$$

Here, k_0 is the reference wave vector and $\omega_0 = k_0 v_0$ is the resonance condition to be used instead of the precessional resonance of Eq. (A.16) with $\ell = 0$. Thus, Eq. (38) is completed by the mapping of resonant denominators

$$n\bar{\omega}_d - \omega_0 \simeq n\bar{\omega}_{d0} \frac{(r - r_0)}{L_{d0}} \leftrightarrow k_0(v - v_0) = k_0 u , \quad (39)$$

where L_{d0} is the characteristic length of variation of $\bar{\omega}_d$ § and $u \equiv (v - v_0)$.

Introducing a source term $Q(v)$ and a simple Krook collision operator, $-\nu(v)f(v)$, the Vlasov equation for a 1D uniform plasma equilibrium is written as

$$d_t f(v) = Q(v) - \nu(v)f(v) . \quad (40)$$

The configuration to velocity space mapping of Eqs. (38) and (39), thus, allows to rewrite Eqs. (36) and (37) as

$$\begin{aligned} (-i\omega + \nu)\delta\hat{f}_0(\omega) = & i\frac{e^2 k_0^2}{m^2} \frac{\partial}{\partial u} \iint_{-\infty}^{\infty} \left[\delta\hat{\phi}_{k_0}(y) \frac{-\partial_u \hat{F}_0(\omega - y - y')}{y - k_0 u - \omega - i\nu} \delta\hat{\phi}_{-k_0}(y') \right. \\ & \left. - \delta\hat{\phi}_{-k_0}(y) \frac{\partial_u \hat{F}_0(\omega - y - y')}{y + k_0 u - \omega - i\nu} \delta\hat{\phi}_{k_0}(y') \right] dy dy' , \quad (41) \end{aligned}$$

when expressed for the nonlinear deviation $\delta\hat{f}_0(\omega)$ of the particle distribution function from the equilibrium (initial) value $F_0(0) = Q(v)/\nu(v)$. Following Ref. [24, 25], it is possible to show that, in the case of many waves characterized by a broad frequency

§ Note that Eq. (38) implies that directions of incrementing v corresponds to decreasing r and vice versa. However, $\bar{\omega}_d$ is also a generally decreasing function of r .

spectrum with overlapping resonances, Eq. (41) reduces to the quasilinear theory of a weakly turbulent plasma [121, 122]. In the opposite limit of a narrow frequency spectrum of nearly periodic nonlinear fluctuations (cf. Sec. 5.3), Eq. (41) describes the oscillations of particles that are trapped in the wave, which, however, do not decay in time as expected as consequence of phase mixing. Therefore, the scalar field $\delta\phi_{k_0}$ oscillations are also predicted to continue indefinitely rather than to fade away, as in actual physical conditions [123], due to the fact that the processes described in Fig. 4 do not account for k_0 -harmonics generation produced by spatial bunching [124].

Equation (41) can also be used to analyze the adiabatic frequency chirping ($|\dot{\omega}| \ll \omega_B^2$) of phase space hole-clump pairs due to the balance of EP power extraction by PSZS with a fixed background dissipation [81, 82, 83, 84, 125]. In particular, two limiting cases have been investigated in the literature: (i) the $\omega_B t \ll 1$ limit [81, 82, 83], where a recursive solution can be adopted near marginal stability; and (ii) the $\omega_B t \gg 1$ limit [84, 125], where the lowest order solution corresponds to a constant distribution function inside the wave-particle trapping separatrix (hole/clump), which is slowly shifting in velocity space (chirping). The recursive solution of Refs. [81, 82, 83], obtained for $\omega_B t \ll 1$, corresponds to taking $\hat{F}_0(\omega - y - y') = i(2\pi)^{-1} F_0(0)(\omega - y - y')^{-1}$ in Eq. (41); *i.e.*, to considering only the first loop in the Dyson series, schematically shown in Fig. 4. Moving to the t -representation, the recursive solution of Eq. (41) is then obtained as

$$\left(\frac{\partial}{\partial t} + \nu\right) \delta f_0 = i \frac{e^2 k_0^2}{m^2} \frac{\partial}{\partial u} \iint_{-\infty}^{\infty} e^{-i(y+y')t} \left[\delta\hat{\phi}_{k_0}(y) \frac{\partial_u F_0(0)}{y' + k_0 u + i\nu} \delta\hat{\phi}_{-k_0}(y') + \delta\hat{\phi}_{-k_0}(y) \frac{\partial_u F_0(0)}{y' - k_0 u + i\nu} \delta\hat{\phi}_{k_0}(y') \right] dy dy' , \quad (42)$$

which is readily cast as

$$\left(\frac{\partial}{\partial t} + \nu\right) \delta f_0 = \frac{\omega_B^2(t)}{4k_0^2} \frac{\partial}{\partial u} \int_0^t \left[e^{-(\nu + ik_0 u)(t-t')} + c.c. \right] \omega_B^2(t') \frac{\partial F_0(0)}{\partial u} dt'. \quad (43)$$

This equation coincides with the evolution equation of PSZS given by Ref. [81], noting that we have introduced $\omega_B^4 \equiv 4(e/m)^2 k_0^4 |\delta\phi_{k_0}|^2$, in order to preserve the same normalizations of Fourier amplitudes used in the original work. The resulting PSZS dynamics can be shown to admit fixed point solutions, nonlinear oscillations as well as finite time singularities [81, 82, 83] (cf. Ref. [72] for a recent review). This latter case, obtained for sufficiently low collisionality, corresponds to breaking down of the truncation in the perturbation expansion of the Dyson series [27]; and coincides with the formation of hole/clump pairs, demonstrated in numerical simulations [126, 127, 128, 129]. The analytic description of adiabatic chirping of hole/clump pairs [84, 125], valid for $\omega_B t \gg 1$ and for isolated PSZS with frequency separation much larger than ω_B , shows that the EP distribution function is flattened (in a coarse-grain sense [130]) inside the wave-particle trapping region. Meanwhile, the energy transfer from EP to PSZS during the chirping process is balanced by fixed background dissipation; that is, the condition under which fluctuations are maintained near marginal stability during the adiabatic evolution of hole/clump structures. These

features are embedded in the general solution of Eq. (41), which, as noted above, can address wave-particle trapping as the shortest time scale nonlinear dynamics [24, 25]. Thus, Eq. (41) can reproduce both $\omega_B t \ll 1$ [81, 82, 83] and $\omega_B t \gg 1$ limits [84, 125]; and addresses the general $\omega_B t \sim 1$ case, where formation of PSZS is expected [27] (cf. Sec. 3).

5.3. Dyson equation for nearly periodic fluctuations

The same results that hold for Eq. (41) with broad and narrow frequency spectrum fluctuations can be obtained for Eq. (36), given the mapping of Eqs. (38) and (39). Thus, one can demonstrate, respectively, quasilinear transport in the radial direction in the case of overlapping resonances, and nonlinear oscillations due to wave-particle trapping in the presence of a nearly periodic large amplitude wave^{||}. Further to this, Eq. (36) can address the onset of nonlocal behaviors in EP transport, including effects of equilibrium geometries and plasma nonuniformity discussed in Sec. 2, which are expected to become progressively more important for increasing EP drive and non-perturbative response [27]. The present approach also shows that, even in the perturbative EP local limit and given the mapping of Eqs. (38) and (39), some features remain in the “fishbone” paradigm that make it qualitatively but not quantitatively the same as the “bump-on-tail” paradigm. For example, the energy dependence of $\bar{\omega}_d$ and $\hat{\omega}_{dn}$ give a different weighting of the particle phase space contributing to the resonant mode drive with respect to the uniform plasma case.

Equation (36), when applied to many modes, provides a framework to explore the transition of EP transports through stochasticity threshold with all the necessary physics ingredients for a realistic comparison with experimental observations and for applications to the dense SAW/DAW fluctuation spectrum typical of fusion plasmas, since it addresses resonance detuning and radial decoupling in wave-particle interactions on the same footing. Equation (36), meanwhile, specialized to nearly periodic fluctuations, can be adopted for nonlinear analyses of “fishbone” oscillations as well as EPMs (cf. Sec. 6).

Given a nearly periodic fluctuation $\delta\bar{\phi}_n(t)$ (spatial dependences are left implicit for the sake of notation simplicity), defined in Eq. (28) and with oscillation frequency centered about $\omega_0(\tau) = \omega_{0r}(\tau) + i\gamma_0(\tau)$ (slowly varying in time), we can write $\delta\bar{\phi}_n(t) \equiv \lim_{\tau \rightarrow t} \delta\bar{\varphi}_n(\tau) \exp(-i\omega_0(\tau)t)$, with $\delta\bar{\varphi}_n(\tau) \equiv \delta\bar{\phi}_{n0} \exp[-i \int_0^\tau \omega_0(t') dt' + i\omega_0(\tau)\tau]$. Thus, as shown in Appendix C, $\delta\bar{\phi}_n(t)$ admits the Laplace transforms

$$\delta\hat{\bar{\phi}}_n(\omega) = \frac{i}{2\pi} \frac{\delta\bar{\varphi}_n(r, \tau)}{\omega - \omega_0(\tau)}, \quad \text{and} \quad \delta\hat{\bar{\phi}}_{-n}(\omega) = \frac{i}{2\pi} \frac{\delta\bar{\varphi}_{-n}(r, \tau)}{\omega + \omega_0^*(\tau)}, \quad (44)$$

provided that $|t - \tau| \lesssim \tau_{NL} \sim |\gamma_0|^{-1}$; and $|\dot{\omega}_{0r}| \ll |\gamma_0 \omega_{0r}|$, $|\dot{\gamma}_0| \ll |\gamma_0^2|$. Therefore, Eq. (44)

^{||} A proof of this can be found, *e.g.*, in the Lectures on *Nonlinear dynamics of phase-space zonal structures and energetic particle physics in fusion plasmas*, F. Zonca, Institute for Fusion Theory and Simulation, Zhejiang University, May 5-16, (2014); http://www.afs.enea.it/zonca/references/seminars/IFTS_spring14.

applies in general to adiabatic as well as non-adiabatic frequency chirping modes. When substituted back into Eq. (36), Eq. (44) yields the following form of the Dyson equation

$$\begin{aligned} \hat{F}_0(\omega) = & \frac{i}{\omega} \text{St} \hat{F}_0(\omega) + \frac{i}{\omega} \hat{S}_0(\omega) + \frac{i}{2\pi\omega} \bar{F}_0(0) + \frac{e}{m} \frac{nc}{\omega(d\psi/dr)} \\ & \times \frac{\partial}{\partial r} \left\{ \left[\frac{Q_{n,\omega_0(\tau)}^*}{\omega_0^*(\tau)} \frac{\hat{F}_0(\omega - 2i\gamma_0(\tau))}{\omega - \omega_0(\tau) + n\bar{\omega}_d} + \frac{Q_{n,\omega_0(\tau)}}{\omega_0(\tau)} \right. \right. \\ & \left. \left. \times \frac{\hat{F}_0(\omega - 2i\gamma_0(\tau))}{\omega + \omega_0^*(\tau) - n\bar{\omega}_d} \right] \hat{\omega}_{dn} |\delta\bar{\varphi}_n(r, \tau)|^2 \right\} , \end{aligned} \quad (45)$$

where $Q_{n,\omega_0(\tau)} \hat{F}_0$ can be approximated by Eq. (37).

Equation (45) is the renormalized form of PSZS generated by nearly periodic fluctuations, which allows investigating the self-consistent nonlinear evolution of SAW/DAW and EP PSZS when “closed” by Eqs. (18) (dropping the ZS shearing effect $\propto \partial_r \langle \delta L_g \rangle_z$) and (25). A crucial element, here, is the different argument of \hat{F}_0 on the LHS and RHS of Eq. (45), since it bears the information on the self-consistent interplay of nonlinear mode dynamics and EP transport. Assuming $|\omega| \gg |\gamma_0| \rightarrow 0$; *i.e.*, assuming fixed amplitude fluctuations, allows to solve Eq. (45) in the uniform radial limit and to recover nonlinear oscillations due to wave-particle trapping, discussed above in this section. In general, however, we have $|\omega| \sim |\gamma_0|$, and Eq. (45) describes much richer dynamics, among which those to be discussed in Sec. 6.

6. EPM convective amplification and avalanches

We analyze the nonlinear dynamics of a nearly periodic EPM burst using Eqs. (18), (25) and (45). In particular, we consider a radially localized EPM wave-packet with perpendicular wavelength $\lambda_\perp \ll L_{EP}$, with L_{EP} the characteristic EP pressure scale length. Furthermore, the mode frequency is assumed to be near the lower accumulation point of the TAE frequency gap in the SAW continuum (cf. also Sec. 3). Thus, $\theta_{k0} = 0$ and $\partial D_n^L / \partial \theta_{k0} = 0$ in Eq. (25) [63, 64, 75, 76, 93]; and

$$\Lambda_n^L \equiv \Lambda_T = (1/2)[(\omega^2 - \omega_\ell^2)/(\omega_u^2 - \omega^2)]^{1/2} . \quad (46)$$

Here, the subscript T stands for “toroidal”; and ω_ℓ/ω_u are the lower/upper SAW continuum accumulation point frequency. Using a simple (s, α) model for high aspect ratio ($R_0/a \gg 1$) tokamak equilibria with circular shifted magnetic flux surfaces [131], with $s \equiv rq'/q$ the magnetic shear and $\alpha \equiv -R_0 q^2 \beta'$ the “ballooning” dimensionless pressure gradient parameter, it is possible to show [63, 64, 132]

$$\delta \bar{W}_{fn}^L = \frac{|s|\pi}{8} \left(1 + 2\kappa(s) - \frac{\alpha}{\alpha_c} \right) ; \quad \text{and} \quad \frac{1}{2} \frac{\partial^2 D_n^L}{\partial \theta_{k0}^2} = \frac{|s|\pi}{8} \kappa(s) , \quad (47)$$

for $|s|, |\alpha| < 1$ in Eq. (25), with $\alpha_c = s^2/(1+|s|)$ and $\kappa(s) \simeq (1/2)(1+1/|s|) \exp(-1/|s|)$. Meanwhile, consistent with the “fishbone” paradigm (cf. Sec. 5), $\delta \bar{W}_{kn}$ can be written

as [27, 63, 64]

$$\begin{aligned} \delta\bar{W}_{kn} = & \int \mathcal{E} d\mathcal{E} d\lambda \sum_{v_{\parallel}/|v_{\parallel}|=\pm} \frac{\pi^2 q R_0}{c^2 k_{\vartheta}^2 |s|} \frac{e^2}{m} \left(\frac{\tau_b n^2 \bar{\omega}_d^2}{\omega_0(\tau)} \right) \\ & \times \int_{-\infty}^{+\infty} \frac{\omega + \omega_0(\tau)}{n\bar{\omega}_d - \omega_0(\tau) - \omega} e^{-i\omega\tau} Q_{n,\omega_0(\tau)} \hat{F}_0(\omega) d\omega, \end{aligned} \quad (48)$$

where $\lambda = \mu B_0/\mathcal{E}$, $\tau_b = 2\pi/\omega_b$, $k_{\vartheta} = -nq/r$, and we have further assumed that magnetically trapped EPs are characterized by harmonic motion between magnetic mirror points; *i.e.*, they are deeply trapped, such that $\hat{\omega}_{dn} \simeq n\bar{\omega}_d$ in Eq. (35). The linear contribution $\delta\bar{W}_{kn}^L$ is readily obtained from Eq. (48) by substitution of $\hat{F}_0(\omega) = (2\pi\omega)^{-1}i\bar{F}_0(0)$, as suggested by Eq. (45). In this case, we assume an initial (equilibrium) EP isotropic slowing down distribution function of particles born at energy E_F . Thus,

$$\bar{F}_0(0) = \frac{3P_{0EP}}{4\pi E_F} \frac{H(E_F/m_{EP} - \mathcal{E})}{(2\mathcal{E})^{3/2} + (2E_c/m_{EP})^{3/2}}; \quad (49)$$

where H denotes the Heaviside step function and the normalization condition is chosen such that the EP energy density is $(3/2)P_{0EP}$ for $E_F \gg E_c$, and EP energy is predominantly transferred to thermal electrons by collisional friction [133] as it occurs for α -particles in fusion plasmas. We then obtain

$$\delta\bar{W}_{kn}^L(\omega_0) = \frac{3\pi(r/R_0)^{1/2}}{8\sqrt{2}|s|} \alpha_{EP} \left[1 + \frac{\omega_0}{\bar{\omega}_{dF}} \ln \left(\frac{\bar{\omega}_{dF}}{\omega_0} - 1 \right) + i\pi \frac{\omega_0}{\bar{\omega}_{dF}} \right], \quad (50)$$

where $\alpha_{EP} = -8\pi R_0 q^2 P'_{0EP}/B_0^2$ and $\bar{\omega}_{dF} = n\bar{\omega}_d(\mathcal{E} = E_F/m_{EP})$. Considering a radially localized EP source, $\alpha_{EP} = \alpha_{0EP} \exp[-(r - r_0)^2/L_{EP}^2]$ [35]; and using Eqs. (46), (47) and (50), it is possible to show that the linear EPM wave-packet, obtained as solution of Eq. (25), has a characteristic radial envelope width $\sim |L_{EP}/k_{\vartheta}|^{1/2}$, with $\lambda_{\perp} \sim |k_{\vartheta}|^{-1} \ll |L_{EP}/k_{\vartheta}|^{1/2} \ll L_{EP}$, consistent with the initial assumptions. Most important, however, is that resonant EPM-EP interactions play a double role: (i) they give mode drive in excess of the local threshold condition set by SAW continuum damping, $\propto \Lambda_T(\omega_{0r})$ [56]; and (ii) they provide the radial potential well that allows EPM to be radially bounded and excited as absolute instability [64, 93]. These properties of resonant EPM-EP interactions are both crucial to explain and understand the nonlinear dynamics of an EPM burst. In fact, they suggest that EPM mode structures may adapt to the nonlinearly modified EP source; and, *vice versa*, that self-consistent evolution of EP PSZS and EPM mode structures may take the form of avalanches [15, 35]. It is, thus, reasonable to seek solutions representing the nearly periodic EPM burst as radially localized, traveling and convectively amplified wave-packets [27].

It is possible to demonstrate that nonlinear dynamics of EP PSZS and EPM are dominated by $\delta\bar{W}_{kn}^{NL}$. In fact, EP effects Λ_n^{NL} are negligible due to finite orbit averaging in the kinetic/inertial layer, while $\delta\bar{W}_{fn}^{NL}$ accounts for non-resonant EP responses [27, 63, 64]. Thus, in the present analysis we may assume $\Lambda_n^{NL} = \delta\bar{W}_{fn}^{NL} = 0$. We further set $S_n^{\text{ext}}(r, t) = 0$ in Eq. (25); and neglect source and collision terms in Eq. (45),

as our aim is to investigate the nonlinear evolution of one single EPM burst excited by the initial unstable distribution given in Eq. (49). By direct substitution into Eq. (48) of $\hat{F}_0(\omega)$ from Eq. (45), and keeping the leading order terms in the time scale ordering of Eq. (2), we obtain

$$\delta\bar{W}_{kn}^{NL} \simeq - \int \mathcal{E} d\mathcal{E} d\lambda \sum_{v_{\parallel}/|v_{\parallel}|=\pm} \frac{\pi^2 q R_0}{c^2 k_{\vartheta}^2 |s|} \frac{e^2}{m} \int_{-\infty}^{+\infty} \frac{\tau_b n^2 \bar{\omega}_d^2(k_{\vartheta}/\Omega) e^{-i\omega t}}{(n\bar{\omega}_d - \omega_{0r}) - i(\gamma_0 - i\omega)} \times \frac{\partial^2}{\partial r^2} \left[\frac{c^2 k_{\vartheta}^2}{B_0^2} \frac{(2i/\omega)(\gamma_0 + i\omega)}{(n\bar{\omega}_d - \omega_{0r})^2 + (\gamma_0 + i\omega)^2} |\delta\bar{\varphi}_n(r, \tau)|^2 \frac{\partial}{\partial r} \hat{F}_0(\omega - 2i\gamma_0) \right] d\omega. \quad (51)$$

Note that, here, we have taken into account that nonlinear EPM dynamics occurs on meso-scales, intermediate between $\lambda_{\perp} \sim |k_{\vartheta}|^{-1}$ and L_{EP} , to have ∂_r commute with quantities that vary on the equilibrium length scale.

In Eq. (51), in addition to the resonant denominators, the integrand has two complex- ω dependences that predominantly contribute to the overall integral value: one is connected with the $\propto 1/\omega$ dependence; the other one is due to the nearly singular/peaked structure of $\hat{F}_0(\omega - 2i\gamma_0)$ at $\omega = 2i\gamma_0$. Due to the $\propto \exp(-i\omega t)$ dependence of the Laplace integrand, the contribution from $\omega \simeq 0$ is exponentially smaller than that from $\omega \simeq 2i\gamma_0$ in the growth and saturation phases of the burst; and is, thus, negligible. This further demonstrates the importance of the self-consistent interplay of nonlinear mode dynamics and EP transport, already noted in Sec. 5.3. Equation (51) also illuminates the competition of phase locking and wave-particle trapping. In fact, noting that the radially localized EPM wave-packet travels at the group velocity v_g , there results a relationship between the wave-packet radial position and its time evolving frequency. Thus, focusing on meso-scale radial structures of the integrand in Eq. (51), at the leading order we can rewrite

$$\frac{\partial_r^2(\dots)}{(n\bar{\omega}_d - \omega_{0r}) - i(\gamma_0 - i\omega)} = \frac{\partial^2}{\partial r^2} \left[\frac{(\dots)}{(n\bar{\omega}_d - \omega_{0r}) - i(\gamma_0 - i\omega)} \right] + 2 \frac{(n\partial_r \bar{\omega}_d - \dot{\omega}_{0r}/v_g) - i\dot{\gamma}_0/v_g}{[(n\bar{\omega}_d - \omega_{0r}) - i(\gamma_0 - i\omega)]^2} \partial_r(\dots) - 2 \frac{[(n\partial_r \bar{\omega}_d - \dot{\omega}_{0r}/v_g) - i\dot{\gamma}_0/v_g]^2}{[(n\bar{\omega}_d - \omega_{0r}) - i(\gamma_0 - i\omega)]^3} (\dots) + \frac{(n\partial_r^2 \bar{\omega}_d - \ddot{\omega}_{0r}/v_g^2) - i\ddot{\gamma}_0/v_g^2}{[(n\bar{\omega}_d - \omega_{0r}) - i(\gamma_0 - i\omega)]^2} (\dots). \quad (52)$$

Noting that $|(n\bar{\omega}_d - \omega_{0r})| \sim |(\gamma_0 - i\omega)| \sim |k_r v_g| \sim \tau_{NL}^{-1}$; and consistent with the time scale ordering of Eq. (2) and discussed after Eq. (44), the dominant contributions on the RHS of Eq. (52) are given by the first three lines, where terms $\propto \dot{\gamma}_0$ and $\propto \ddot{\gamma}_0$ can be dropped. Meanwhile, given Eq. (A.35) for $\ell = 0$, the contribution of second and third line on the RHS are, respectively $\sim |\tau_{NL}^2 \ddot{\mathbf{O}}_{m,n,\ell=0}|$ and $\sim |\tau_{NL}^4 \ddot{\mathbf{O}}_{m,n,\ell=0}|^2$ w.r.t. the first line. These terms are generally important, and, in the “bump-on-tail” paradigm or the uniform plasma limit for SAW/DAW near marginal stability (cf. Sec. 5), account for wave-particle trapping [24, 25]. However, when phase locking occurs, Eq. (A.42),

second and third line on the RHS of Eq. (52) become negligible, consistent with Eq. (6). Thus, phase locking *de facto* prevents wave-particle trapping to occur (cf. Appendix A.3). Note also that $|\tau_{NL}^2 \ddot{\Theta}_{m,n,\ell=0}| \sim \epsilon_{\bar{\omega}} \ll 1$ by definition, Eq. (A.45). Thus, on time scales shorter than $\epsilon_{\bar{\omega}}^{-1} \tau_{NL}$, Eq. (52) with only the first line on the RHS can be used to calculate $\delta \bar{W}_{kn}^{NL}$, which describes convective amplification of a nearly periodic phase locked EPM burst when substituted back into Eq. (25). Phase locking, Eq. (A.42), assumed here as a simplifying Ansatz, can be self-consistently verified *a posteriori*, once the solution is obtained as shown below. On longer time scales, wave-particle trapping and/or resonance detuning must be accounted for, along with non-resonant EP responses as well as collisions and other relevant phenomena, neglected here but discussed in Ref. [15].

For the phase locked EPM, the velocity space integral of Eq. (51) is dominated by resonant particles and by $\omega \simeq 2i\gamma_0$, as discussed above. Thus, noting that $n\bar{\omega}_d \simeq -k_{\vartheta} \mathcal{E}/(R_0 \Omega)$ and $\tau_b \simeq 2\pi q R_0 (R_0/r)^{1/2} \mathcal{E}^{-1/2}$ for the simplified equilibrium considered in this section [64], Eq. (51) can be reduced to [27] ¶

$$\begin{aligned} \delta \bar{W}_{kn}^{NL} \simeq & -i \frac{8\pi^4 E_F}{|s| B_0^2} \frac{\omega_{0r}}{\bar{\omega}_{dF}} \left(\frac{r}{R_0} \right)^{1/2} q^2 R_0 \frac{\partial^2}{\partial r^2} \int_{-\infty}^{+\infty} \left[\frac{c^2 k_{\vartheta}^2}{B_0^2} \frac{|\delta \bar{\phi}_n(r, t)|^2}{(2\gamma_0 - i\omega)^2} \right. \\ & \times \left. \frac{\partial}{\partial r} \left(\mathcal{E}^{3/2} \hat{F}_0(\omega) \right)_{n\bar{\omega}_d = \omega_{0r}} \right] e^{-i\omega t} d\omega = -i \frac{8\pi^4 E_F}{|s| B_0^2} \frac{\omega_{0r}}{\bar{\omega}_{dF}} \left(\frac{r}{R_0} \right)^{1/2} \\ & \times q^2 R_0 \frac{\partial^2}{\partial r^2} \partial_t^{-2} \left[\frac{c^2 k_{\vartheta}^2}{B_0^2} |\delta \bar{\phi}_n(r, t)|^2 \frac{\partial}{\partial r} (\mathcal{E}^{3/2} F_0(t))_{n\bar{\omega}_d = \omega_{0r}} \right]. \quad (53) \end{aligned}$$

Furthermore, following Ref. [35] and noting that the analysis is limited to times shorter than $\epsilon_{\bar{\omega}}^{-1} \tau_{NL}$, $F_0(t) \simeq \bar{F}_0(0)$ with $\bar{F}_0(0)$ given by Eq. (49). Thus, Eq. (51) can be further simplified and yields

$$\delta \bar{W}_{kn}^{NL} \simeq i \text{Im} [\delta \bar{W}_{kn}^L(\omega_{0r})] k_{\vartheta}^2 \rho_{EP}^2 v_{EP}^2 \partial_t^{-2} \partial_r^2 |\bar{A}_{n0}(r, t)|^2, \quad (54)$$

where $v_{EP}^2 = E_F/m_{EP}$, $\rho_{EP}^2 = v_{EP}^2/\Omega_{EP}^2$, $\text{Im} [\delta \bar{W}_{kn}^L(\omega_{0r})]$ is given by Eq. (50), and we have introduced the normalized amplitude [27]

$$(e_{EP}/E_F) \delta \bar{\phi}_n(r, t) = \bar{A}_n(r, t) = e^{-i\omega_{0r} t} \bar{A}_{n0}(r, t). \quad (55)$$

Collecting terms, the desired nonlinear evolution equation for $\bar{A}_{n0}(r, t)$, Eq. (25), can then be rewritten as

$$\begin{aligned} & [i (\Lambda_T(\omega_{0r}) - \text{Im} [\delta \bar{W}_{kn}^L(\omega_{0r})]) - (\delta \bar{W}_{fn}^L + \text{Re} [\delta \bar{W}_{kn}^L(\omega_{0r})])] \bar{A}_{n0} \\ & = \left[\frac{\partial \text{Re} [\delta \bar{W}_{kn}^L(\omega_{0r})]}{\partial \omega_{0r}} \left(i \frac{\partial}{\partial t} \right) + \frac{1}{2k_{\vartheta}^2 s^2} \frac{\partial^2 D_n^L}{\partial \theta_{k0}^2} \frac{\partial^2}{\partial r^2} \right. \\ & \quad \left. + i \text{Im} [\delta \bar{W}_{kn}^L(\omega_{0r})] k_{\vartheta}^2 \rho_{EP}^2 v_{EP}^2 \partial_t^{-2} \frac{\partial^2}{\partial r^2} |\bar{A}_{n0}|^2 \right] \bar{A}_{n0}, \quad (56) \end{aligned}$$

¶ Note, here, that Eq. (53) assumes $\text{Res} (\hat{F}_0(\omega)|_{n\bar{\omega}_d = \omega_{0r}}, 0) = (2\pi i)^{-1} \oint_{\Gamma_r} \hat{F}_0(\omega; z) dz = 0$, with $z \equiv (n\bar{\omega}_d/\omega_{0r} - 1)$ and Γ_r a vanishing circular path in the complex- z plane centered at $z = 0$. In the general case, an expression for $\delta \bar{W}_{kn}^{NL}$ can still be written but is slightly more complicated. For the application discussed here, Eq. (53) is adequate.

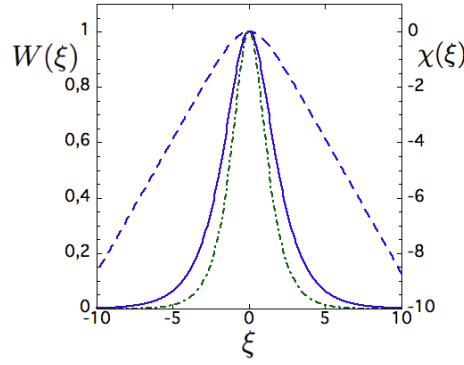


Figure 5. Normalized amplitude, $W(\xi)$ (solid blue line), and phase, $\chi(\xi)$ (dashed blue line), of the nonlinear EPM wave-packet. The function $\text{sech}(\xi)$ (green dash-dotted line) is also shown as reference.

where all contributions are defined in Eqs. (46), (47) and (50).

Equation (56) readily recovers the linear limit [64, 93]. In the general case [27, 63], as suggested by the last term on the RHS, Eq. (56) is a nonlinear Schrödinger equation describing the evolution of the nearly periodic phase locked EPM burst in an “active medium”. We can look for solutions in the convectively amplified self-similar form [27]

$$\bar{A}_{n0}(r, t) = U(\xi) \exp \int_0^t \gamma_0(t') dt' = W(\xi) \exp \left(i\chi(\xi) + \int_0^t \gamma_0(t') dt' \right), \quad (57)$$

with

$$\xi \equiv k_{n0} \left(r - r_0 - \int_0^t v_g(t') dt' \right), \quad (58)$$

and k_{n0} denoting the nonlinear radial wave vector. Noting that $\partial_r \bar{A}_{n0} = k_{n0} \partial_\xi U(\xi) \exp \int_0^t \gamma_0(t') dt'$ and $\partial_t \bar{A}_{n0} = (\gamma_0 - k_{n0} v_g \partial_\xi) U(\xi) \exp \int_0^t \gamma_0(t') dt'$, there exist two regimes in the nonlinear EPM burst evolution: (i) $\gamma_0 \gtrsim |k_{n0} v_g|$, where the linear EPM is increasingly modified by the nonlinear interplay with EP transport as the fluctuation intensity increases; and (ii) $\gamma_0 < |k_{n0} v_g|$, where the nonlinear EPM-EP interaction dominates the dynamics. In this second case, it is possible to solve Eq. (56) in a simple analytical form. In fact, balancing the nonlinear term with the linear dispersiveness in Eq. (56) yields

$$v_g = \lambda_g \hat{v}_{EP}^{E \times B}, \quad \text{and} \quad k_{n0}^2 = \frac{k_\vartheta^2 s^2 \text{Im} [\delta \bar{W}_{kn}^L(\omega_{0r})]}{\lambda_g^2 \partial^2 D_n^L / \partial \theta_{k0}^2}, \quad (59)$$

with $\hat{v}_{EP}^{E \times B} = (-k_\vartheta c / B_0) \max[\delta \bar{\phi}_n(r, t)]$ the radial $\mathbf{E} \times \mathbf{B}$ velocity at the fluctuation peak, λ_g an $\mathcal{O}(1)$ control parameter to be determined; and

$$\partial_\xi^2 U = \lambda_0 U - 2iU|U|^2, \quad (60)$$

where $\lambda_0 \simeq -0.47 + i1.33$ corresponds to the ground state of the complex nonlinear oscillator described by Eq. (60), whose numerical solution is shown in Fig. 5, separating amplitude and phase, $U(\xi) = W(\xi)e^{i\chi(\xi)}$. With this solution, Eq. (56) becomes the

“nonlinear” EPM dispersion relation

$$D_n^{L\ell}(\omega_0) - \frac{\lambda_0}{2\lambda_g^2} \mathbb{Im} [\delta \bar{W}_{kn}^L(\omega_{0r})] = 0 \quad , \quad (61)$$

where

$$\begin{aligned} D_n^{L\ell}(\omega_0) = & i \left(\Lambda_T(\omega_{0r}) - \mathbb{Im} [\delta \bar{W}_{kn}^L(\omega_{0r})] \right) - (\delta \bar{W}_{fn}^L + \mathbb{Re} [\delta \bar{W}_{kn}^L(\omega_{0r})]) \\ & - \left(\omega_{0r} \frac{\partial \mathbb{Re} [\delta \bar{W}_{kn}^L(\omega_{0r})]}{\partial \omega_{0r}} \right) i \frac{\gamma_0}{\omega_{0r}} \end{aligned} \quad (62)$$

is the linearized “local” EPM dispersion function [56], obtained neglecting the linear dispersiveness $\propto \partial^2 D_n^L / \partial \theta_{k0}^2$ [64].

Equations (59) and (61) describe a one-parameter family, λ_g , of possible EPM wave-packets that are convectively amplified as they radially propagate with a group velocity $\propto \hat{v}_{EP}^{E \times B}$. The dominant nonlinear mode is obtained for

$$\frac{d\gamma_0}{d\lambda_g^2} = \frac{\partial \gamma_0}{\partial \lambda_g^2} + \frac{\partial \gamma_0}{\partial \omega_{0r}} \frac{d\omega_{0r}}{d\lambda_g^2} = 0 \quad ; \quad (63)$$

i.e., for maximized mode growth and wave-EP power transfer [27]. For typical tokamak plasma parameters, and the simplified model plasma equilibrium adopted here, one generally finds $\lambda_g \simeq 0.5 \div 0.6^+$. Thus, the EPM wave-packet propagates radially at a substantial fraction of the peak EP $\mathbf{E} \times \mathbf{B}$ velocity and, as a result, resonant EP motion is predominantly ballistic in the radial direction, similar to the “mode particle pumping” mechanism introduced in Ref. [16] for explaining EP secular loss due to “fishbones”. Equation (61) applies at the instantaneous radial position $r_1(t) = r_0 + \int_0^t v_g(t') dt'$ of the EPM wave-packet. The dependence on r_1 , in the present model equilibrium, is explicit in terms $\propto \alpha_{EP}$ and $\propto \bar{\omega}_{dF}$; and implicit in terms depending on ω_0 . Due to the $\propto \ln(\bar{\omega}_{dF}/\omega_0 - 1)$ term and $\omega_0/\bar{\omega}_{dF}$ dependences of $\delta \bar{W}_{kn}^L$ in Eq. (50), the real EPM frequency is given by

$$\omega_{0r}/\bar{\omega}_{dF}(r_1) \simeq \text{const} \quad , \quad (64)$$

at the leading order, so that the phase locking condition, Eqs. (6) and (A.42), is readily satisfied, consistent with the Ansatz and introductory discussions above in this section. Meanwhile, since $\mathbb{Im} \lambda_0 > 0$, the nonlinear EPM-EP interplay results into a strengthening of the mode drive w.r.t. the linear value $\propto \mathbb{Im} [\delta \bar{W}_{kn}^L(\omega_{0r})]$. Thus, the convective amplification of the phase locked EPM is an “avalanche” [35]; and wave-packet amplification can continue until quenched by radial nonuniformities; *i.e.*, the combined effect of decreasing values of linear drive $\mathbb{Im} [\delta \bar{W}_{kn}^L(\omega_{0r})] \propto \alpha_{EP}$ and increasing values of SAW continuum damping $\propto \Lambda_T(\omega_{0r})$ (cf. Secs. 2.2 and Appendix A.3; and Refs. [15, 26, 27]). Hence, as consequence of phase locking, meso-scale nonlinear dynamics of the EPM burst as well as EP transport are extended to the macro-scales.

The self-consistent interplay of nonlinear EPM radial structure evolution with EP transport suggests that this is a non-adiabatic “autoresonance” effect (cf.

⁺ It is possible to verify that $d\gamma_0/d\lambda_g^2 > 0$ for $\lambda_g^2 \rightarrow 0$, and $d\gamma_0/d\lambda_g^2 < 0$ for $\lambda_g^2 \rightarrow \infty$.

Sec. 2.2), caused by the non-perturbative EP response and the ensuing kinetic EPM dispersiveness. Plasma instability and non-perturbative EP behavior are the crucial differences with respect to adiabatic “autoresonance”, where fluctuations are driven/controlled externally and adiabatic frequency sweeping is imposed [54, 55]. During the amplification process and non-adiabatic frequency chirping, the relevant nonlinear time scale is $\tau_{NL} \sim |\partial_t^{-1}| \sim |A_{n0}|^{-1}$, consistent with Eq. (59). Furthermore, since $v_g = \lambda_g \hat{v}_{EP}^{E \times B}$, the EPM intensity is proportional to the square of the traveled distance, similar to the propagation of a FEL short optical pulse in the superradiant regime [62]. Similar to superradiance is also the resonant EPM-EP interaction, which takes place when the wave-EP phase is amplifying due to the phase locking condition. By the time residual resonance detuning changes the wave-EP phase to damping, the resonance condition is lost by radial decoupling. Thus, EPMs can be considered as examples of “autoresonance” and “superradiance” in fusion plasmas [27, 134]. Other interesting analogies with neighboring research areas are further discussed in Ref. [27]. For example, Eq. (60) shows interesting analogies with $\partial_\xi^2 U = U - 2U^3$ yielding $U = \text{sech}(\xi)$; *i.e.*, the equation of motion of a nonlinear oscillator in the so-called “Sagdeev potential” $V = (-U^2 + U^4)/2$, which can be obtained, *e.g.*, in the analysis of Ion Temperature Gradient turbulence spreading via soliton formation [114], but also from the Gross-Pitaevsky equation, describing the ground state of a quantum system of identical bosons [135, 136]; and from the investigation of the envelope of modulated water wave groups [137]. However, Eq. (60) maintains its peculiarities, mostly due to its complex nature coming from the self-consistent interplay of EPM radial structure and EP transport.

7. Summary and Discussions

Phase space zonal structures play fundamental roles in EP transport induced by SAW/DAW instabilities with $|\gamma_L/\omega_0| \ll 1$ in burning fusion plasmas. In this work, we have derived general equations that can be used as starting point in analytic as well as numerical investigations of the self-consistent interplay of SAW/DAW instabilities and PSZS in the presence of a non-perturbative EP population in fusion plasmas with realistic equilibrium geometry and plasma nonuniformities. As particular case of the general equations, we have derived a reduced description that may be adopted for nearly periodic fluctuations within the “fishbone” paradigm; and applied it to the analytic study of convective EPM amplification as solitons in active media. Phase locking, in this case, extends the meso-scale dynamics of EPM “avalanches” and causes secular EP redistribution on the macro-scales. These processes have interesting analogies with “autoresonance” in nonlinear dynamics and “superradiance” in FEL operations.

The strength of the instability drive controls the mechanism by which nonlinear saturation is reached in nonuniform plasma equilibria and realistic magnetic field geometries. The reduced 1D uniform plasma description, adopted in the “bump-on-tail” paradigm, applies near marginal stability as long as the nonlinear particle displacement

at saturation is significantly smaller than the radial mode width. As a result, mode saturation occurs via wave-particle trapping and resonance detuning. For sufficiently strong EP drive, $|\gamma_L/\omega_0| > |\gamma_L/\omega_0|_c$ ($|\gamma_L/\omega_0|_c \lesssim 10^{-2}$ for typical parameters), the fluctuation induced EP displacement becomes comparable to the radial mode width, and radial decoupling of EPs from mode structures is increasingly more important in the nonlinear saturation dynamics, until it eventually dominates over resonance detuning. This transition is demonstrated in numerical simulation experiments of meso-scale dynamics of EPs; and is indicative of the plasma behavior as a 3D system, with given equilibrium geometry and plasma nonuniformity. Restricting the analysis to precessional resonance with magnetically trapped particles only, the general case can be reduced to a 1D nonuniform plasma, adopted in the “fishbone” paradigm, which recovers the “bump-on-tail” paradigm in the uniform plasma limit; and allows to understand the onset of non-local behaviors, such as self-consistent interplay of mode structures and EP transport.

The strength of instability drive or, more precisely, the perturbative vs. non-perturbative EP behavior, also controls the frequency dynamics of PSZS. Very near SAW/DAW marginal stability, such that the “bump-on-tail” paradigm can be applied, wave-particle trapping is the fastest nonlinear time scale and, for sufficiently weak collisions, PSZS may evolve into hole/clump pairs with adiabatically sweeping frequency ($|\dot{\omega}| \ll \omega_B^2$), which are maintained near marginal stability by balancing energy extraction from EP phase space with background dissipation. Meanwhile, for sufficiently strong EP drive that the “fishbone” paradigm must be adopted and EP response is non-perturbative, kinetic SAW/DAW dispersiveness, self-consistently modified by EP transport, causes non-adiabatic frequency evolution ($|\dot{\omega}| \sim \omega_B^2$). Phase locked resonant EPs dominate nonlinear dynamics and, by reduction of resonance detuning, nonlinear interplay of secular EP transport with radial mode structures becomes the most important nonlinear physics.

The present theoretical framework, conceived and developed for application to SAW/DAW instabilities in burning fusion plasmas with a non-perturbative EP population, is characterized by the peculiar system geometry and equilibrium non-uniformity. However, it also sheds light on physics aspects that may be of relevance to neighboring fields of research, such as space plasma physics, nonlinear dynamics, condensed matter and accelerator physics.

Acknowledgments

This work was supported by European Unions Horizon 2020 research and innovation program under grant agreement number 633053 as Enabling Research Project CfP-WP14-ER-01/ENEA_Frascati-01; and by US DoE, ITER-CN, and NSFC No. 11235009 grants.

Appendix A. Wave particle interactions in axisymmetric toroidal systems.

For gyrokinetic theory in axisymmetric toroidal systems, considered in this work, two obvious pairs of action angle coordinates for charged particle motions are $(m\mu, \alpha)$, with $\mu = v_\perp^2/(2B_0) + \dots$ the magnetic moment (see, *e.g.*, Refs. [60, 138]) and α the gyrophase; and (P_ϕ, ϕ) , with P_ϕ the canonical toroidal angular momentum and ϕ the toroidal angle^{*}. Here, perpendicular (\perp) and parallel (\parallel) directions are defined with respect to the unit vector $\mathbf{b} = \mathbf{B}_0/B_0$; and the axisymmetric equilibrium magnetic field configuration is assumed in the form

$$\mathbf{B}_0 = F(\psi)\nabla\phi + \nabla\phi \times \nabla\psi ; \quad (\text{A.1})$$

$2\pi\psi$ denoting the poloidal magnetic flux within the magnetic surface labeled by ψ . Consistent with the main text, we adopt field aligned toroidal flux coordinates (r, θ, ζ) , with $r = r(\psi)$ a radial-like flux variable, the poloidal angle θ is chosen such that the Jacobian $\mathcal{J} = (\nabla\psi \times \nabla\theta \cdot \nabla\zeta)^{-1}$ satisfies the condition $\mathcal{J}B_0^2$ being a magnetic flux function [139, 140]; and the general toroidal angle $\zeta \equiv \phi - \nu(\psi, \theta)$, $\nu(\psi, \theta)$ being a suitable periodic function of θ [141], such that the safety factor q ,

$$q = \frac{\mathbf{B}_0 \cdot \nabla\zeta}{\mathbf{B}_0 \cdot \nabla\theta} = q(\psi) , \quad (\text{A.2})$$

is a function of ψ . At the leading order, P_ϕ is given by

$$P_\phi = \frac{e}{c} \left(F(\psi) \frac{v_\parallel}{\Omega} - \psi \right) ; \quad (\text{A.3})$$

with $\Omega = eB_0/(mc)$ the cyclotron frequency. The third pair of action angle coordinates is (J, θ_c) , with J the “second invariant” and θ_c the respective conjugate canonical angle

$$J = \oint v_\parallel dl , \quad \theta_c = \omega_b \int_0^\theta d\theta' / \dot{\theta}' . \quad (\text{A.4})$$

Here, integrals are taken along the particle orbits in the equilibrium magnetic field, dl denoting the arc-length element along it; and we have introduced the unified notation ω_b for bounce and transit frequency of trapped and circulating particles, respectively,

$$\omega_b(\mu, J, P_\phi) = \frac{2\pi}{\oint d\theta / \dot{\theta}} . \quad (\text{A.5})$$

Given $H_0 = m(v_\parallel^2 + \mu B_0)$ and the definitions of J and ω_b ,

$$\frac{\partial J}{\partial H_0} = \frac{2\pi}{\omega_b} \leftrightarrow \omega_b = 2\pi \frac{\partial H_0}{\partial J} .$$

Therefore, J can be readily computed given the reference magnetic equilibrium

$$J = J(\mu, P_\phi, H_0) \leftrightarrow H_0 = H_0(\mu, J, P_\phi) .$$

^{*} A recent review of coordinates systems and their connection with the description of the guiding-center particle motion is given by Cary and Brizard [138].

Equation (A.4) yields $\theta_c = \omega_b \tau$, with τ a time-like parameter tracking the particle position along the closed poloidal orbit of period $2\pi/\omega_b$. Thus, for a particle with given constants of motion,

$$r = \bar{r} + \tilde{\rho}_c(\theta_c) \quad , \quad (\text{A.6})$$

where \bar{r} and $\tilde{\rho}_c(\theta_c)$ are parameterized by (μ, J, P_ϕ) and the initial particle radial position[‡]; and “tilde” denotes a generic periodic function in θ_c with zero average, which can be computed from the particle equations of motion in the equilibrium \mathbf{B}_0 . Similarly, it is readily demonstrated that, for circulating particles (*i.e.*; particles whose $v_{||}$ does not change sign)

$$\theta = \theta_c + \tilde{\Theta}_c(\theta_c) \quad , \quad (\text{A.7})$$

while, for magnetically trapped particles (*i.e.*; particles whose $v_{||}$ changes sign twice along a closed orbit in the (r, θ) plane),

$$\theta = \tilde{\Theta}_c(\theta_c) \quad . \quad (\text{A.8})$$

Note, again, that $\tilde{\Theta}_c$ is a periodic function of θ_c with zero average, which is parameterized by (μ, J, P_ϕ) . Thus it takes different values in Eqs. (A.7) and (A.8). At last, considering Eqs. (A.2) and the definition of $\zeta \equiv \phi - \nu(\psi, \theta)$, the parametric representation of ζ along the particle orbit in the equilibrium \mathbf{B}_0 is

$$\zeta = \bar{\omega}_d \tau + \bar{q} \theta + \tilde{\Xi}_c(\theta_c) \quad . \quad (\text{A.9})$$

Here, θ is given by Eqs. (A.7) or (A.8), $\bar{\omega}_d(\mu, J, P_\phi)$ is the toroidal precession frequency and

$$\bar{q}(\mu, J, P_\phi) = \frac{\oint q d\theta}{\oint d\theta} = \frac{\oint q \dot{\theta} d\theta_c}{\oint \dot{\theta} d\theta_c} \quad . \quad (\text{A.10})$$

Note that, even though q does not depend on θ , it depends on the particle position because of the particle radial displacement. Meanwhile, from Eq. (A.9) and (A.10), one readily derives the following definition for the toroidal precession frequency

$$\bar{\omega}_d(\mu, J, P_\phi) = \frac{\omega_b}{2\pi} \oint \left(\dot{\zeta} - q \dot{\theta} \right) \frac{d\theta}{\dot{\theta}} \quad . \quad (\text{A.11})$$

Appendix A.1. Wave particle resonance condition

Using Eqs. (A.6) to (A.9), the Fourier decomposition

$$f(r, \theta, \zeta) = \sum_{m,n \in \mathbb{Z}} e^{in\zeta - im\theta} f_{m,n}(r) \quad (\text{A.12})$$

of a scalar function $f(r, \theta, \zeta)$, describing a generic fluctuating field for which time dependence has been left implicit, can be projected along the unperturbed particle motion in the equilibrium \mathbf{B}_0 using the time-like parameter $\tau = \theta_c/\omega_b$; expressing (r, θ, ζ)

[‡] The initial particle poloidal angle can be reabsorbed by suitable time shift in the time-like parameter τ ; *i.e.*, in θ_c .

in terms of the particle position along its unperturbed trajectory. More specifically, we have

$$f(r, \theta, \zeta) = \sum_{m, n, \ell \in \mathbb{Z}} e^{i(n\bar{\omega}_d + \ell\omega_b)\tau} \mathcal{P}_{m, n, \ell} \circ f_{m, n}(\bar{r}) . \quad (\text{A.13})$$

Here, we have introduced the projection operators along the particle motion in the equilibrium \mathbf{B}_0 , defined as

$$\mathcal{P}_{m, n, \ell} \circ f_{m, n}(\bar{r}) \equiv \frac{\lambda_{m, n}}{2\pi} \oint \exp \left\{ in\tilde{\Xi}_c(\theta_c) + i[n\bar{q}(\bar{r}) - m]\tilde{\Theta}_c(\theta_c) \right\} f_{m, n}(\bar{r} + \tilde{\rho}_c(\theta_c)) e^{-i\ell\theta_c} d\theta_c . \quad (\text{A.14})$$

Furthermore, $\lambda_{m, n} = 1$ for magnetically trapped particles, while, for circulating particles,

$$\lambda_{m, n} = \exp[i(n\bar{q}(\bar{r}) - m)\omega_b\tau] . \quad (\text{A.15})$$

Note that Eq. (A.13) represents the value of $f(r, \theta, \zeta)$ effectively experienced by the particle along its orbit, parameterized by the actions (μ, J, P_ϕ) , or equivalently by (μ, P_ϕ, H_0) (see above), and by the time-like variable $\tau = \theta_c/\omega_b$. The integer $\ell \in \mathbb{Z}$ stands for the “bounce harmonic”, similarly to $m, n \in \mathbb{Z}$ denoting poloidal and toroidal Fourier harmonics. Equation (A.13) is completely defined, together with the functions $\tilde{\Theta}_c(\theta_c)$, $\tilde{\Xi}_c(\theta_c)$ and $\tilde{\rho}_c(\theta_c)$ that are obtained from the integration of particle motion, once the reference equilibrium \mathbf{B}_0 is assigned. This mode structure decomposition corresponds to a “Lagrangian” description of the fluctuation while moving in the reference frame of the considered particle; *i.e.*, it is a lifting of a generic scalar field to the particle phase space [27]. Meanwhile, Eq. (A.12) is the usual mode structure decomposition of the fluctuating field in the laboratory frame. These two descriptions are the basis of the dual nature of fluctuation structures within a kinetic analysis of wave particle interactions: one with emphasis on the “effective” fluctuation strength experienced by the particles; and another one, reflecting the fields measured by the “observer”. Of these two descriptions, the former enters in the resonant particle dynamic response and, thus, is crucially important for wave-particle power exchange, resonant excitation and instability drive; and particle transports [18]. The latter, meanwhile, is what enters in the evolution equation(s) for the mode structures.

As noted above, time dependences in $f(r, \theta, \zeta)$ are left implicit to simplify notation. Once a monochromatic wave $f(r, \theta, \zeta) \propto \exp(-i\omega_0 t)$ is assumed, the resonance condition; *i.e.*, the stationarity of wave-particle phase in the particle moving frame where $\tau \leftrightarrow t$, is readily derived from Eq. (A.13) and yields

$$\omega_0 = \omega_0(\mu, J, P_\phi) = n\bar{\omega}_d + \ell\omega_b \quad (\text{A.16})$$

for magnetically trapped particles; while, for circulating particles,

$$\omega_0 = \omega_0(\mu, J, P_\phi) = n\bar{\omega}_d + \ell\omega_b + (n\bar{q}(\bar{r}) - m)\omega_b . \quad (\text{A.17})$$

Here, we remind that ω_b stands for both bounce and transit frequencies. We also note that $\bar{\omega}_d$ is typically negligible for circulating particles, except for particles that are close to the trapped-to-circulating boundary in the action space.

Appendix A.2. The effect of fluctuations

When considering the effect of fluctuations, for every bounce/transit; *i.e.*, a 2π increment in the angle θ_c , a shift will be accumulated in the wave-particle phase (“resonance detuning”), because of radial nonuniformities and the dependence of $\bar{\omega}_d$ and ω_b on J, P_ϕ that are not conserved anymore in the nonlinear regime (μ is conserved for low frequency fluctuations, analyzed here, for which $|\omega_0| \ll |\Omega|$). Moreover, the wave-particle phase in the mode structure decomposition in action-angle variables will also be shifted, since $\tilde{\Theta}_c(\theta_c)$, $\tilde{\Xi}_c(\theta_c)$ and $\tilde{\rho}_c(\theta_c)$ are not simple periodic functions of θ_c any longer, as in the given plasma equilibrium. Consistent with the time scale ordering assumed in this work and, in particular, with the condition $1 \gg |\omega_0 \tau_{NL}|^{-1} \sim |\gamma_L/\omega_0| \gg \epsilon_\omega \equiv |\omega_0/\Omega|$ (cf. Sec. 2), we assume that for every bounce/transit the effect of the nonlinear dynamics is small compared with the oscillations of the equilibrium particle trajectory. However, the cumulative effect of the nonlinear dynamics on many bounce/transit times can be large and even connected with a secular process; *i.e.*, not bounded in time.

The perturbed equations of motion, which are needed to extend Eq. (A.13) to handle the effect of small but finite amplitude fluctuations, can be readily obtained from the expression of the gyrocenter Hamiltonian up to order $\sim \epsilon_\delta \equiv |\delta \mathbf{B}_\perp/B_0| \ll 1$ [60]; yielding the expressions for $\delta \dot{r}$ ($\delta \dot{\psi}$), $\delta \dot{\theta}$ and $\delta \dot{\zeta}$, as well as for \dot{H}_0 , \dot{P}_ϕ and \dot{J} . Here, $(\delta r, \delta \theta, \delta \zeta)$ denote the change in particle position due to the small but finite amplitude fluctuations, which are also the cause of δH_0 , δP_ϕ and δJ and finite \dot{H}_0 , \dot{P}_ϕ and \dot{J} . All these perturbed quantities are considered here to be formally linear in the fluctuation fields. Within this level of approximation of gyrokinetic description of particle motions, the conserved invariants are μ and the extended phase space Hamiltonian $K = H_0 + e \langle \delta \phi_g - v_\parallel \delta A_{\parallel g}/c \rangle - \bar{H}$ (cf., *e.g.*, [70, 142]), whose conservation can be readily cast as

$$\frac{\partial}{\partial t} \dot{\Pi}_\phi + \frac{\partial}{\partial \zeta} \dot{\bar{H}} = 0 . \quad (\text{A.18})$$

Here, \bar{H} is the gyrocenter Hamiltonian up to order $\sim \epsilon_\delta$ [60]

$$\bar{H} = H_0 + e \langle \delta \phi_g \rangle - e \frac{v_\parallel}{c} \langle \delta A_{\parallel g} \rangle ; \quad (\text{A.19})$$

and Π_ϕ is the extension of the canonical toroidal angular momentum, Eq. (A.3), in the presence of fluctuations and for \mathbf{B}_0 expressed as in Eq. (A.1),

$$\Pi_\phi = P_\phi + \frac{e F(\psi)}{c B_0} \langle \delta A_{\parallel g} \rangle . \quad (\text{A.20})$$

Furthermore, it is readily shown that, for trapped particles, we have

$$\theta = \tilde{\Theta}_c(\theta_c) + \Delta\theta , \quad (\text{A.21})$$

while, for circulating particles,

$$\begin{aligned} \theta = & \omega_b \tau + \tilde{\Theta}_c(\theta_c) + \Delta\theta \\ & + \frac{\partial \omega_b}{\partial P_\phi} \int_0^\tau \delta P_\phi d\tau' + \frac{\partial \omega_b}{\partial J} \int_0^\tau \delta J d\tau' , \end{aligned} \quad (\text{A.22})$$

with

$$\Delta\theta = \int_0^\tau \delta\dot{\theta} \frac{d\theta}{\dot{\theta}} . \quad (\text{A.23})$$

Note that the difference between Eqs. (A.21) and (A.22) stems from the different nature of unperturbed orbits, respectively described by Eqs. (A.8) and (A.7), and from the varied expression of $\theta_c \rightarrow \theta_c + \delta\theta_c$ ($\delta\theta_c = \int_0^\tau \delta\omega_b d\tau'$) for circulating particles in the presence of fluctuations. Similarly, the radial motion is described as

$$r = \bar{r} + \tilde{\rho}_c(\theta_c) + \Delta r , \quad (\text{A.24})$$

$$\Delta r = \int_0^\tau \delta\dot{r} \frac{d\theta}{\dot{\theta}} , \quad (\text{A.25})$$

while ζ is given by

$$\begin{aligned} \zeta &= \bar{\omega}_d \tau + \bar{q} \theta + \tilde{\Xi}_c(\theta_c) + \Delta\zeta \\ &\quad + \frac{\partial \bar{\omega}_d}{\partial P_\phi} \int_0^\tau \delta P_\phi d\tau' + \frac{\partial \bar{\omega}_d}{\partial J} \int_0^\tau \delta J d\tau' \end{aligned} \quad (\text{A.26})$$

$$\begin{aligned} &\quad + \bar{q} \left(\frac{\partial \omega_b}{\partial P_\phi} \int_0^\tau \delta P_\phi d\tau' + \frac{\partial \omega_b}{\partial J} \int_0^\tau \delta J d\tau' \right) + \omega_b \frac{d\bar{q}}{d\bar{r}} \int_0^\tau \delta r d\tau' , \\ \Delta\zeta &= \int_0^\tau \delta\dot{\zeta} \frac{d\theta}{\dot{\theta}} . \end{aligned} \quad (\text{A.27})$$

Here, the terms involving ω_b and its derivatives with respect to P_ϕ and J are to be considered for circulating particles only. In fact, these terms are originated by the effect of fluctuations on the term $\propto \bar{q}\theta_c = \int_0^\tau \omega_b \bar{q} d\tau'$, due to the unperturbed circulating particle motion, Eq. (A.7), which has no correspondence in the unperturbed trapped particle motion, Eq. (A.8). In particular, terms $\propto \partial\omega_b/\partial P_\phi, \partial\omega_b/\partial J$ have the same origin of those included in Eq. (A.22) for circulating particles and excluded in Eq. (A.21) for magnetically trapped particles. Similarly, the term involving $\sim \omega_b(d\bar{q}/d\bar{r})$ stems from $\int_0^\tau \omega_b \delta\bar{q} d\tau'$ for circulating particles only.

With the above results, we can extend the mode structure decomposition in action-angle variables, Eq. (A.13), to include nonlinear particle orbit distortions due to fluctuations:

$$f(r, \theta, \zeta) = \sum_{m,n,\ell \in \mathbb{Z}} \lambda_{m,n}^{NL} e^{i(n\bar{\omega}_d + \ell\omega_b)\tau + i\Theta_{m,n,\ell}^{NL}} \mathcal{P}_{m,n,\ell} \circ e^{\Delta r \partial_{\bar{r}}} f_{m,n}(\bar{r}) , \quad (\text{A.28})$$

where $\mathcal{P}_{m,n,\ell} \circ e^{\Delta r \partial_{\bar{r}}} f_{m,n}$ is defined as in Eq. (A.14), $\lambda_{m,n}^{NL}$ is the nonlinear extension of Eq. (A.15), *i.e.*, $\lambda_{m,n}^{NL} = 1$ for trapped particles, while for circulating particles

$$\begin{aligned} \lambda_{m,n}^{NL} &= \exp \left[i(n\bar{q}(\bar{r}) - m) \left(\frac{\partial \omega_b}{\partial P_\phi} \int_0^\tau \delta P_\phi d\tau' \right. \right. \\ &\quad \left. \left. + \frac{\partial \omega_b}{\partial J} \int_0^\tau \delta J d\tau' \right) + in\omega_b \frac{d\bar{q}}{d\bar{r}} \int_0^\tau \delta r d\tau' \right] ; \end{aligned} \quad (\text{A.29})$$

and the definition of $\Theta_{m,n,\ell}^{NL}$ is

$$\Theta_{m,n,\ell}^{NL} = n\Delta\zeta - m\Delta\theta + n \left(\frac{\partial \bar{\omega}_d}{\partial P_\phi} \int_0^\tau \delta P_\phi d\tau' + \frac{\partial \bar{\omega}_d}{\partial J} \int_0^\tau \delta J d\tau' \right)$$

$$+ \ell \left(\frac{\partial \omega_b}{\partial P_\phi} \int_0^\tau \delta P_\phi d\tau' + \frac{\partial \omega_b}{\partial J} \int_0^\tau \delta J d\tau' \right) . \quad (\text{A.30})$$

Equation (A.28) can be rewritten in a more compact form, introducing the definition

$$\Theta_{m,n,\ell} \equiv \Theta_{m,n,\ell}^{NL} - i \ln \lambda_{m,n}^{NL} - \int_0^\tau \Delta \omega(t) dt , \quad (\text{A.31})$$

so that the nonlinear frequency shift $\Delta \omega(t) = \omega(t) - \omega_0$ for a nearly monochromatic wave (cf. Sec. 5.3) is explicitly taken into account, leaving implicit only the time dependence of the reference linear instability. Note that the concept of nearly monochromatic wave still applies for frequency chirping modes as long as $|\dot{\omega}| = |\Delta \dot{\omega}| \ll |\gamma_L \omega_0|$; *i.e.*, for both adiabatic ($|\dot{\omega}| \ll \omega_B^2$) and non-adiabatic ($|\dot{\omega}| \lesssim \omega_B^2$) frequency sweeping, ω_B denoting the wave-particle trapping frequency. Meanwhile, we have, at the lowest order,

$$\mathcal{P}_{m,n,\ell} \circ e^{\Delta r \partial_r} f_{m,n}(\bar{r}) \simeq \mathcal{P}_{m,n,\ell} \circ f_{m,n}(\bar{r} + \Delta r) ; \quad (\text{A.32})$$

with Δr being the bounce-averaged nonlinear radial particle displacement, accumulated over many bounces/transits (2π increments in θ_c). For each bounce/transit, the bounce-averaging involved in the definition of $\mathcal{P}_{m,n,\ell} \circ f_{m,n}(\bar{r})$, Eq. (A.14), is carried out at the “effective” \bar{r} location shifted by the accumulated bounce-averaged nonlinear radial particle displacement. Therefore, Eq. (A.28) can be finally cast as

$$f(r, \theta, \zeta) = \sum_{m,n,\ell \in \mathbb{Z}} e^{i(n\bar{\omega}_d + \ell\omega_b)\tau + i\Theta_{m,n,\ell}} \mathcal{P}_{m,n,\ell} \circ f_{m,n}(\bar{r} + \Delta r) . \quad (\text{A.33})$$

Thus, the dominant effect of nonlinear physics on wave-particle resonances enters via the nonlinear phase shift $\Theta_{m,n,\ell}$ (“resonance detuning”) and/or the $\mathcal{P}_{m,n,\ell} \circ f_{m,n}(\bar{r} + \Delta r)$ functions (“radial decoupling”), which regulate the strength of wave-particle resonances due to the radial mode structure. In both cases, these processes can be understood as cumulative effects of bounce-averaged responses on linear particle motions. This viewpoint is very useful when describing wave-particle interactions by Hamiltonian techniques; *e.g.*, by “kinetic Poincaré plots” introduced recently by White [99]. Meanwhile, a rather detailed analysis, based on implementation of Hamiltonian phase space diagnostics, aimed at investigating the relative importance of “resonance detuning” vs. “radial decoupling” in numerical simulations of nonlinear dynamics of SAW excited by EPs, is given in Ref. [53].

Appendix A.3. Finite interaction length and finite interaction time

By direct inspection of Eqs. (A.29) and (A.30), it is readily recognized that resonance detuning is drastically different for circulating particle and trapped particle resonances. In fact, from EP equations of motion and Eq. (A.18) one generally has $\Delta r/r \sim \Delta P_\phi/P_\phi \sim (\omega_{*EP}/\omega_0)\Delta H_0/H_0$ [27, 106], with ω_{*EP} the EP diamagnetic frequency. Thus, not only radial decoupling but also resonance detuning for EPs is expected to be dominated by the nonlinear radial displacement, since $|\omega_{*E}/\omega_0| \gg 1$ for SAW excited by EPs in fusion plasmas. Let us also consider high- n toroidal mode number modes, as expected in ITER [63, 64], and moderate/low bounce harmonics; *i.e.*, $\ell = \mathcal{O}(1)$.

Specializing, for simplicity, to the case of a toroidal equilibrium with major radius R_0 and shifted circular magnetic surfaces, we readily obtain

$$\dot{\Theta}_{m,n,l} \simeq n \frac{d\bar{q}}{dr} \omega_t \Delta r - \Delta\omega \quad , \quad (\text{A.34})$$

for circulating particles, having denoted the transit frequency as ω_t and neglected $\bar{\omega}_d$; whereas, for magnetically trapped particle resonance,

$$\dot{\Theta}_{m,n,l} \simeq \left(n \frac{\partial \bar{\omega}_d}{\partial \bar{r}} + \ell \frac{\partial \bar{\omega}_b}{\partial \bar{r}} \right) \Delta r - \Delta\omega \quad . \quad (\text{A.35})$$

Meanwhile, for both circulating and magnetically trapped particles, the equation for Δr is

$$\begin{aligned} \Delta \dot{r} \simeq & i \frac{c}{B_0} \sum_{m,n,\ell \in \mathbb{Z}} \frac{n\bar{q}}{\bar{r}} e^{i(n\bar{\omega}_d + \ell\bar{\omega}_b)\tau + i\Theta_{m,n,\ell}} \\ & \times \mathcal{P}_{m,n,\ell} \circ \left\langle \frac{\bar{r}q}{r\bar{q}} \left[1 - \frac{v_{\parallel}}{qR_0\omega} (nq - m) \right] \delta\phi_g \right\rangle_{m,n} (\bar{r} + \Delta r) \quad , \quad (\text{A.36}) \end{aligned}$$

having used $\delta A_{\parallel m,n} \simeq (nq - m)/(qR_0)(c/\omega)\delta\phi_{m,n}$; *i.e.*, $\delta E_{\parallel} \simeq 0$ at the lowest order for SAW. For a resonance given by Eqs. (A.16) or (A.17), Eqs. (A.34) to (A.36) may describe an isolated resonance as well as resonance overlap in the case of many modes. It is also worthwhile emphasizing that, for the same toroidal mode number n , different poloidal mode numbers m are generally coherent, since they belong to the same (generally nonlinear) mode structure. From Eqs. (A.34) to (A.36) with $\Delta\omega = 0$, the wave-particle trapping frequency ω_B is readily estimated as

$$\omega_B^2 \simeq \lambda_n \left| \frac{\omega}{r} \delta \dot{\mathbf{X}}_{\perp} \right| \simeq \lambda_n \left| \frac{\omega}{r} \frac{nq}{r} \frac{c}{B_0} \delta\phi \right| \quad , \quad (\text{A.37})$$

with $\lambda_n = |nrq'|$ for circulating, $\lambda_n = 1$ for magnetically trapped particles; and $\delta \dot{\mathbf{X}}_{\perp}$ the fluctuating $\mathbf{E} \times \mathbf{B}$ guiding-center drift velocity [60, 138]. In the derivation of Eq. (A.37), the estimate $d_{tt}\Delta r \sim \omega_B^2 \Delta r$ has been adopted, and resonant particles have been assumed; *i.e.*, Eq. (A.16) for magnetically trapped and Eq. (A.17) for circulating particles, respectively. Given ω_B , the separatrix width in particle phase space, Δr_{sx} , is estimated as $\Delta r_{sx} \simeq |\delta \dot{\mathbf{X}}_{\perp} / \omega_B|$. Thus, Δr_{sx} and ω_B are of order $\sim \epsilon_{\delta}^{1/2}$.

Equations (A.34) and (A.35) can be used for estimating the finite interaction length and finite interaction time for resonant particles; *i.e.*, the typical spatial and time scales required for particles to effectively loose the resonance condition in a non-uniform system. For $\Delta\omega = 0$; *i.e.*, no frequency chirping, the finite interaction time for resonant particles defines the characteristic nonlinear time scale and is given by

$$\dot{\Theta}_{m,n,\ell} \tau_{NL} \sim 1 \quad ; \quad \text{and} \quad \tau_{NL} \sim 1/(3\gamma_L) \quad . \quad (\text{A.38})$$

Note that the γ_L^{-1} enters via the anticipated saturation process (either resonance detuning or radial decoupling; or both, with varying relative weight); *i.e.*, saturation occurs when $\tau_{NL} \sim 1/(3\gamma_L)$. Here, the factor 3 is a typical value adopted from analyses of the beam-plasma system [143, 144], as well as numerical simulations of

Alfvén Eigenmodes (AE) in toroidal plasmas [145]. Meanwhile, neglecting the radial mode structure, the finite interaction length, Δr_L , is obtained from Eq. (A.34) as

$$3\gamma_L \sim nq'\omega\Delta r_L \quad (\text{A.39})$$

for circulating particles; while, from Eq. (A.35),

$$3\gamma_L \sim \omega(\Delta r_L/r) \quad (\text{A.40})$$

for magnetically trapped particles; where characteristic radial scale lengths of ω_t , $\bar{\omega}_d$ and ω_b are taken to be $\sim r$. From these estimates, we readily recognize that the finite interaction length, Δr_L , for circulating resonant particles is typically smaller than the characteristic width, $\sim |nq'|^{-1}$ [63, 64, 111], of one poloidal harmonic, $\delta\phi_{m,n}$; whereas it may be comparable or larger than $\sim |nq'|^{-1}$ for magnetically trapped resonant particles if $(\gamma_L/\omega) \gtrsim |3nrq'|^{-1}$. For high- n modes as expected in ITER [63, 64], this condition is $(\gamma_L/\omega) \gtrsim 10^{-2}$. Thus, circulating particles transport due to isolated resonances is predicted to be local, causing minor radial profile relaxation, while transport is expected to be mostly diffusive in the presence of many modes [27]. Meanwhile, magnetically trapped EP transports is intrinsically non-local; *i.e.*, characterized by meso-scales, larger than $|nq'|^{-1}$ and shorter than the equilibrium scale length, and convective (ballistic) processes [27]. Different trapped particle vs. circulating particle behaviors are very general, as they are connected with the properties of Eqs. (A.34) and (A.35), and are expected to play important role whenever resonant particle transport is significant. In fact, both convective and diffusive electron motion have been reported in gyrokinetic numerical simulations of collisionless trapped electron mode turbulence [146]. Ballistic and (super/sub) diffusive EP behaviors have also been demonstrated in the presence of interchange turbulence in simple magnetized toroidal plasmas [147, 148]; and, more recently, diffusive circulating particle transport vs. ballistic magnetically trapped particle behaviors induced by electrostatic drift wave turbulence have been discussed in Ref. [149].

Somewhat different behaviors are expected for low- n modes, routinely excited in present day experiments. Here, convective (ballistic) supra-thermal particle transport is observed typically in connection with significant non-adiabatic [$|\dot{\omega}| \lesssim \omega_B^2$; cf. discussions following Eq. (A.31)] frequency sweeping as, *e.g.*, in NSTX experiments with neutral beam injection [150, 151, 152]. Secular radial motions of resonant particles were recognized by White *et al* [16] to be a key mechanism, dubbed “mode particle pumping”, for explaining fishbone nonlinear dynamics [17] and related particle losses. This phenomenology is readily explained by Eqs. (A.34) to (A.36), which have the same structure of the original equations derived in Ref. [16]; and predict secular (ballistic) particle motions if the $\dot{\Theta}_{m,n,\ell} = 0$ resonance condition is preserved as the particles are transported out of the system. In fact, Eqs. (A.39) and (A.40) give “mode particle pumping” by “phase locking” for circulating and magnetically trapped particles when, respectively [16, 153],

$$\Delta\dot{\omega} \simeq n \frac{d\bar{q}}{d\bar{r}} \omega_t \Delta\dot{r} \quad , \quad (\text{A.41})$$

and

$$\Delta\dot{\omega} \simeq \left(n \frac{\partial \bar{\omega}_d}{\partial \bar{r}} + \ell \frac{\partial \bar{\omega}_b}{\partial \bar{r}} \right) \Delta\dot{r} . \quad (\text{A.42})$$

It is worthwhile noting that, because of Eqs. (A.41) and (A.42) together with Eqs. (A.36) and (A.37), “phase locking” and secular (ballistic) particle transport always imply non-adiabatic frequency sweeping, $\Delta\dot{\omega} \sim \omega_B^2$. Another important feature of the phase locking condition and $\Delta\dot{r}$ given by Eq. (A.36) is that the frequency sweeping rate is proportional to the mode amplitude; *i.e.*, it is fastest when the mode is strongest. This is observed in typical experimental conditions, when resonant particle transport is ballistic (see, *e.g.*, Refs. [3, 151]), and in numerical simulations of, *e.g.*, nonlinear EPM evolutions [73, 94, 95, 96, 97, 100] and, more recently, nonlinear fishbone dynamics [50, 154, 155].

The effect of phase locking is to extend the finite interaction lengths, given by Eqs. (A.41) and (A.42) in the $\Delta\omega = 0$ no-frequency sweeping limit, to, respectively

$$3\gamma_L \sim nq'\omega\epsilon_{\dot{\omega}}\Delta r_L , \quad (\text{A.43})$$

and

$$3\gamma_L \sim \omega\epsilon_{\dot{\omega}}(\Delta r_L/r) . \quad (\text{A.44})$$

Here, $\epsilon_{\dot{\omega}}$ is defined as

$$\epsilon_{\dot{\omega}} \equiv \left| \frac{\dot{\Theta}_{m,n,\ell}(\Delta\omega)}{\dot{\Theta}_{m,n,\ell}(\Delta\omega = 0)} \right| , \quad (\text{A.45})$$

where numerator and denominator are computed from Eq. (A.31), respectively, at the actual value of the nonlinear frequency shift (frequency chirping) and at $\Delta\omega = 0$ (no chirping). The value of $\epsilon_{\dot{\omega}}$ denotes the effectiveness of phase locking; it depends on the wave dispersive properties [27] and, in general, $\epsilon_{\dot{\omega}} < 1$ requires the EP dynamics being non-perturbative. A similar argument applies to the finite interaction time, which is also extended by $\sim \epsilon_{\dot{\omega}}^{-1}$. Because of the extended interaction length, circulating resonant particles can also be displaced by a significant fraction of $\sim |nq'|^{-1}$ before resonance detuning sets in. Thus, in the presence of significant non-adiabatic frequency sweeping, circulating EP transports are also expected to occur as convective processes even for long-wavelength modes. This has, indeed, been observed experimentally, *e.g.*, in recent NSTX experiments with neutral beam injection [150, 151]; and in numerical simulations [73, 94, 97, 100], where it is shown that the structure of the SAW continuous spectrum is crucial in the nonlinear mode dynamics and frequency chirping [73, 94, 96, 97, 100, 101, 102, 103, 104].

The secular resonant particle motion, predicted by Eqs. (A.41) and (A.42) is restricted to a group of particles that have similar initial wave-particle phase and can be maintained as long as the mode frequency can be swept preserving phase locking on the one hand and, on the other hand, satisfying the mode dispersion relation. When phase locked resonant particles eventually loose the resonance condition after the finite interaction time/length, they may be substituted by others; and the process can continue

until quenched by equilibrium nonuniformity (cf. Secs. 2.2 and 6; and Refs. [15, 26, 27]). In fact, non-adiabatic frequency sweeping prevents the *de facto* wave-particle trapping to occur and particle can enter and leave the resonant region during the nonlinear evolution, which maximizes wave-particle power exchange as well as mode growth [27] (cf. Sec. 6).

Appendix B. The general fishbone like dispersion relation

Here, expressions for Λ_n , $\delta\bar{W}_{fn}$ and $\delta\bar{W}_{kn}$ to be used in Eq. (23) are given, without derivation, for the readers' convenience. Detailed derivations of these expressions can be found in Refs. [27, 63, 64]. The generalized “inertia”, Λ_n , accounting for the radially local structures of the SAW continuous spectrum, is given by

$$i\Lambda_n \equiv \frac{1}{2} \left(\delta\hat{\Psi}_{-n0+}^\dagger \delta\hat{\Psi}_{n0+} \right)^{-1} \left[\delta\hat{\Psi}_{-n}^\dagger(\vartheta) \partial_\vartheta \delta\hat{\Psi}_n(\vartheta) \right]_{\vartheta \rightarrow 0^-}^{\vartheta \rightarrow 0^+}, \quad (\text{B.1})$$

where $\delta\hat{\Psi}_{n0+} = \lim_{\vartheta \rightarrow 0^+} \delta\hat{\Psi}_n(\vartheta)$, and $\delta\hat{\Psi}_n(\vartheta)$ is obtained from the solution of the short radial scale limit ($k_\perp^2 \simeq k_r^2$) of the gyrokinetic vorticity equation written as [27, 63, 64]

$$\begin{aligned} & \left(\frac{\partial^2}{\partial \vartheta^2} - \frac{\partial_\vartheta^2 \hat{\kappa}_\perp}{\hat{\kappa}_\perp} \right) \delta\hat{\Psi}_n - \frac{\mathcal{J}^2 B_0^2}{v_A^2} \frac{\partial}{\partial t} \left[\frac{\partial}{\partial t} + i\omega_{*pi} \right. \\ & \quad \left. - \frac{3}{4} k_\vartheta^2 \rho_i^2 \hat{\kappa}_\perp^2 \left(\frac{\partial}{\partial t} + i\omega_{*pi} + i\omega_{*Ti} \right) \right] \delta\hat{\Phi}_n \\ & \quad - \lim_{\hat{\kappa}_\perp \rightarrow \infty} \frac{4\pi \mathcal{J}^2 B_0}{ck_\vartheta^2 \hat{\kappa}_\perp} \mathbf{b} \times \boldsymbol{\kappa} \cdot \boldsymbol{\nabla} \sum \left\langle m (\mu B_0 + v_\parallel^2) J_0 \frac{\partial}{\partial t} \delta\hat{g}_n \right\rangle_v \\ & \quad + [\text{NL TERMS}] = 0. \end{aligned} \quad (\text{B.2})$$

Here, we have adopted Eq. (21) for representing spatiotemporal structures of SAW/DAW, $\mathbf{k}_\perp = -i\boldsymbol{\nabla}_\perp$, $\kappa_\perp^2 \equiv \hat{\kappa}_\perp^2 k_\vartheta^2$, $k_\vartheta \equiv -nq/r$, $\delta\hat{\Psi}_n = \hat{\kappa}_\perp \delta\hat{\psi}_n$, $\delta\hat{\Phi}_n = \hat{\kappa}_\perp \delta\hat{\phi}_n$, $\rho_i = (T_i/m_i)^{1/2}/\Omega_i$ is the thermal ion Larmor radius, \mathcal{J} is the Jacobian [cf. Appendix A, following Eq. (A.1)], summation is extended to all particle species, and we have introduced the thermal ion diamagnetic frequencies

$$\begin{aligned} \omega_{*pi} &= \omega_{*ni} + \omega_{*Ti}, \\ \omega_{*ni} &= \left(\frac{T_0 c}{en_0 B_0} \right)_i (\mathbf{b} \times \boldsymbol{\nabla} n_{0i}) \cdot \mathbf{k}_\perp, \\ \omega_{*Ti} &= \left(\frac{c}{eB_0} \right)_i (\mathbf{b} \times \boldsymbol{\nabla} T_{0i}) \cdot \mathbf{k}_\perp. \end{aligned} \quad (\text{B.3})$$

Furthermore, for the sake of simplicity, we have assumed the long wavelength limit $k_\perp^2 \rho_i^2 \ll 1$, except in the magnetic curvature coupling term, where J_0 is maintained for brevity. Interested readers can find a discussion of the more general $k_\perp \rho_i \sim 1$ case in Refs. [27, 63, 64]. Note that the $\sim \delta\hat{g}_n$ term generally includes nonlinear particle response via $\delta\hat{g}_n$ itself. Finally, formally nonlinear terms, denoted as [NL TERMS], are given by

$$[\text{NL TERMS}] = \lim_{\hat{\kappa}_\perp \rightarrow \infty} \frac{\mathcal{J}^2 B_0^2}{k_\vartheta^2 \hat{\kappa}_\perp v_A^2} \frac{\partial^2}{\partial t^2} \mathcal{P}_{Bn} \left(\frac{\delta \varrho_m}{\varrho_{m0}} \nabla_\perp^2 \delta\phi \right), \quad (\text{B.4})$$

$$\begin{aligned}
& - \lim_{\hat{\kappa}_\perp \rightarrow \infty} \frac{\mathcal{J}^2 B_0}{ck_\vartheta^2 \hat{\kappa}_\perp} \mathcal{P}_{Bn} (\mathbf{b} \times \nabla \delta A_\parallel \cdot \nabla \nabla_\perp^2 \delta A_\parallel) \\
& - \lim_{\hat{\kappa}_\perp \rightarrow \infty} \sum_{\neq e} \frac{2\pi e \mathcal{J}^2 B_0^2}{ck_\vartheta^2 \hat{\kappa}_\perp \Omega^2} \mathcal{P}_{Bn} [\mathbf{b} \times \nabla (\nabla_\perp^2 \delta \phi) \cdot \nabla \langle \mu \delta g \rangle_v \\
& - \mathbf{b} \times \nabla \delta \phi \cdot \nabla \langle \mu \nabla_\perp^2 \delta g \rangle_v - \nabla_\perp^2 (\mathbf{b} \times \nabla \delta \phi \cdot \nabla \langle \mu \delta g \rangle_v)] .
\end{aligned}$$

Here, $\delta \varrho_m$ stands for plasma mass density fluctuation about the equilibrium value ϱ_{m0} , summation is extended to all particle species except thermal electrons and, in order to simplify notation, we have introduced the operators \mathcal{P}_{Bn} [63, 64],

$$\mathcal{P}_{Bn}(r, \vartheta) : f(r, \theta, \zeta) \mapsto \hat{f}_n(r, \vartheta) , \quad (\text{B.5})$$

which act on a generic function $f(r, \theta, \zeta)$ in (r, θ, ζ) space, producing the corresponding $\hat{f}_n(r, \vartheta)$ component in (r, ϑ) space, consistent with Eq. (21). In Eq. (B.4), the first line represents the polarization current nonlinearity [130], the second one accounts for the Maxwell stress, while the third line is the kinetic expression representing both nonlinear diamagnetic response and Reynolds stress for $k_\perp^2 \rho_i^2 \ll 1$ [27, 63].

The expressions of $\delta \bar{W}_{fn}$ and $\delta \bar{W}_{kn}$ are obtained by construction of a quadratic form starting from the gyrokinetic vorticity equation [27, 63], and are given by

$$\begin{aligned}
\delta \bar{W}_{nf} + \delta \bar{W}_{nk} = & \left(\delta \hat{\Phi}_{-n0+}^\dagger \delta \hat{\Phi}_{n0+} \right)^{-1} \frac{1}{2} \int_{-\infty}^{\infty} \left[\left(\frac{\partial}{\partial \vartheta} \delta \hat{\Phi}_{-n} \right)^\dagger \left(\frac{\partial}{\partial \vartheta} \delta \hat{\Phi}_n \right) \right. \\
& + \frac{\partial_\vartheta^2 \hat{\kappa}_\perp}{\hat{\kappa}_\perp} \delta \hat{\Phi}_{-n}^\dagger \delta \hat{\Phi}_n + \delta \hat{\Phi}_{-n}^\dagger \frac{\mathcal{J}^2 B_0^2}{v_A^2} \frac{\partial}{\partial t} \left(\frac{\partial}{\partial t} + i\omega_{*pi} \right) \delta \hat{\Phi}_n \\
& \left. + \delta \hat{\Phi}_{-n}^\dagger \frac{4\pi \mathcal{J}^2 B_0}{ck_\vartheta^2 \hat{\kappa}_\perp} \mathbf{b} \times \boldsymbol{\kappa} \cdot \nabla \sum \left\langle m (\mu B_0 + v_\parallel^2) J_0 \frac{\partial}{\partial t} \delta \hat{g}_n \right\rangle_v \right] d\vartheta .
\end{aligned} \quad (\text{B.6})$$

Here, we noted that $\delta \hat{\Phi}_n(\vartheta) \simeq \delta \hat{\Psi}_n(\vartheta)$ for regular SAW/DAW radial structures away from resonances with the SAW continuous spectrum. Furthermore, the nonlinear contribution to $\delta \bar{W}_{nf} + \delta \bar{W}_{nk}$ is mainly due to the $\sim \delta \hat{g}_n$ term, while formally nonlinear terms in the gyrokinetic vorticity equation [cf. Eq. (B.4)] predominantly contribute to Λ_n [27, 63]. The nonlinearity due to EP response in the $\sim \delta \hat{g}_n$ term is what is considered in this work for the analyses of EPM avalanches, carried out in Sec. 6 adopting the “fishbone paradigm” (cf. Sec. 5). The expressions of $\delta \bar{W}_{fn}$ and $\delta \bar{W}_{kn}$ in Eq. (B.6) can be extracted, dividing $\delta \hat{g}_n$ in “fluid” and “kinetic” responses as specified in Eq. (31) [17]. The expression for $\delta \bar{W}_{kn}$ is then obtained from Eq. (B.6) using the “kinetic” response only in the $\sim \delta \hat{g}_n$ term. Note that the remaining $\delta \bar{W}_{fn}$ does not include the (linear) “kink drive” contribution, which is typically negligible for SAW/DAW and can be anyway readily included for application of the present theoretical framework to MHD modes [27, 63, 64].

Appendix C. Laplace transform of nearly periodic fluctuations

In this Appendix, we justify the Laplace representation of Eq. (44) for nearly periodic fluctuations, and discuss its validity in terms of relevant time scales.

Introduce the slow and fast time variables τ and t , with $\tau \simeq t$ but $|\partial_t| \gg |\partial_\tau|$ and $d_t = \partial_t + \partial_\tau$. Furthermore, given a nearly periodic fluctuation $\delta\bar{\phi}_n(t)$ (spatial dependences are left implicit for the sake of notation simplicity), defined in Eq. (28) and with oscillation frequency centered about $\omega_0(\tau) = \omega_{0r}(\tau) + i\gamma_0(\tau)$ (slowly varying in time), we let

$$\begin{aligned}\delta\bar{\phi}_n(t) &\equiv \lim_{\tau \rightarrow t} \delta\varphi_n(t, \tau) \equiv \lim_{\tau \rightarrow t} \delta\bar{\varphi}_n(\tau) \exp(-i\omega_0(\tau)t) \\ \delta\bar{\varphi}_n(\tau) &\equiv \delta\bar{\phi}_{n0} \exp\left[-i \int_0^\tau \omega_0(t') dt' + i\omega_0(\tau)\tau\right] .\end{aligned}\quad (\text{C.1})$$

Noting that

$$(\partial_t + \partial_\tau)\delta\varphi_n(t, \tau) = [-i\omega_0(\tau) + i\dot{\omega}_0(\tau)(\tau - t)]\delta\varphi_n(t, \tau) ,$$

Eq. (C.1) admits the Laplace transforms

$$\hat{\delta\bar{\phi}}_n(\omega) = \frac{i}{2\pi} \frac{\delta\bar{\varphi}_n(r, \tau)}{\omega - \omega_0(\tau)} , \quad \text{and} \quad \hat{\delta\bar{\phi}}_{-n}(\omega) = \frac{i}{2\pi} \frac{\delta\bar{\varphi}_{-n}(r, \tau)}{\omega + \omega_0^*(\tau)} , \quad (\text{C.2})$$

provided that $|t - \tau| \lesssim \tau_{NL} \sim |\gamma_0|^{-1}$; and $|\dot{\omega}_{0r}| \ll |\gamma_0\omega_{0r}|$, $|\dot{\gamma}_0| \ll |\gamma_0^2|$. Thus, considering the time scale ordering of Eq. (2), Eq. (C.2) applies in general to adiabatic as well as non-adiabatic frequency chirping modes; and is adopted in this work as Eq. (44).

References

- [1] Chen L and Zonca F 2007 *Nucl. Fusion* **47** S727
- [2] Fasoli A, Gormezano C, Berk H L, Breizman B N, Briguglio S, Darrow D S, Gorelenkov N N, Heidbrink W W, Jaun A, Konovalov S V, Nazikian R, Noterdaeme J, Sharapov S E, Shinohara K, Testa D, Tobita K, Todo Y, Vlad G and Zonca F 2007 *Nucl. Fusion* **47** S264
- [3] Heidbrink W W 2008 *Phys. Plasmas* **15** 055501
- [4] Belikov V S, Kolesnichenko Ya I and Oraevskij V N 1968 *Zh. Eksp. Teor. Fiz.* **5** 2210
- [5] Belikov V S, Kolesnichenko Ya I and Oraevskij V N 1969 *Sov. Phys. JETP* **28** 1172
- [6] Rosenbluth M N and Rutherford P H 1975 *Phys. Rev. Lett.* **34** 1428
- [7] Mikhailovskii A B 1975 *Sov. Phys. JETP* **41** 890
- [8] Mikhailovskii A B 1975 *Zh. Eksp. Teor. Fiz.* **68** 1772
- [9] Zonca F, Chen L, Dong J Q and Santoro R A 1999 *Phys. Plasmas* **6** 1917
- [10] Nazikian R, Berk H L, Budny R V, Burrell K H, Doyle E J, Fonck R J, Gorelenkov N N, Holcomb C, Kramer G J, Jayakumar R J, La Haye R J, McKee G R, Makowski M A, Peebles W A, Rhodes T L, Solomon W M, Strait E J, Van Zeeland M A and Zeng L 2006 *Phys. Rev. Lett.* **96** 105006
- [11] Hasegawa H and Chen L 1976 *Phys. Fluids* **19** 1924
- [12] Zonca F and Chen L 2008 Nonlinear Dynamics and Complex Behaviors in Magnetized Plasmas of Fusion Interest *Frontiers in Modern Plasma Physics* vol CP1061 ed Shukla P K, Eliasson B and Stenflo L (AIP) p 34
- [13] Zonca F 2008 *Int. J. Mod. Phys. A* **23** 1165
- [14] Qiu Z, Zonca F and Chen L 2012 *Phys. Plasmas* **19** 082507
- [15] Zonca F, Chen L, Briguglio S, Fogaccia G, Milovanov A V, Qiu Z, Vlad G and Wang X 2014 Energetic particles and multi-scale dynamics in fusion plasmas *Plasma Phys. Control. Fusion* to be published
- [16] White R B, Goldston R J, McGuire K, Boozer A H, Monticello D A and Park W 1983 *Phys. Fluids* **26** 2958

- [17] Chen L, White R B and Rosenbluth M N 1984 *Phys. Rev. Lett.* **52** 1122
- [18] Chen L 1999 *J. Geophys. Res.* **104** 2421
- [19] White R B, Gorelenkov N, Heidbrink W W and Van Zeeland M A 2010 *Phys. Plasmas* **17** 056107
- [20] White R B, Gorelenkov N, Heidbrink W W and Van Zeeland M A 2010 *Plasma Phys. Control. Fusion* **52** 045012
- [21] Van Hove L 1955 *Physica* **21** 517
- [22] Prigogine I 1962 *Nonequilibrium Statistical Mechanics* (New York: Interscience)
- [23] Balescu R 1963 *Statistical Mechanics of Charged Particles* (New York: Interscience)
- [24] Al'tshul' L M and Karpman V I 1965 *Zh. Eksp. Teor. Fiz.* **49** 515
- [25] Al'tshul' L M and Karpman V I 1966 *Sov. Phys. JETP* **22** 361
- [26] Zonca F, Briguglio S, Chen L, Fogaccia G, Vlad G and Wang X 2013 Nonlinear dynamics of phase-space zonal structures and energetic particle physics *Proceedings of the 6th IAEA Technical Meeting on "Theory of Plasmas Instabilities"* (Vienna, Austria, May 27 - 29: IAEA, Vienna)
- [27] Chen L and Zonca F 2014 Physics of Alfvén waves and energetic particles in burning plasmas *Rev. Mod. Phys.* submitted
- [28] Hasegawa A, MacLennan C G and Kodama Y 1979 *Phys. Fluids* **22** 2122
- [29] Lin Z, Hahm T S, Lee W W, Tang W M and White R B 1998 *Science* **281** 1835
- [30] Diamond P H, Itoh S-I, Itoh K and Hahm T S 2005 *Plasma Phys. Control. Fusion* **47** R35
- [31] Itoh K, Itoh S-I, Diamond P H, Hahm T S, Fujisawa A, Tynan G R, Yagi M and Nagashima Y 2006 *Phys. Plasmas* **13** 055502
- [32] Taylor J B and McNamara B 1971 *Phys. Fluids* **14** 1492
- [33] Okuda H and Dawson J M 1973 *Phys. Fluids* **16** 408
- [34] Shukla P K, Yu M Y, Rahman H U and Spatschek K H 1984 *Phys. Rep.* **105** 227
- [35] Zonca F, Briguglio S, Chen L, Fogaccia G and Vlad G 2005 *Nucl. Fusion* **45** 477
- [36] Zonca F, Briguglio S, Chen L, Fogaccia G, Hahm T S, Milovanov A V and Vlad G 2006 *Plasma Phys. Control. Fusion* **48** B15
- [37] Chen L and Zonca F 2007 *Nucl. Fusion* **47** 886
- [38] Wang W X, Hahm T S, Lee W W, Rewoldt G, Manickam J and Tang W M 2007 *Phys. Plasmas* **14** 072306
- [39] Dif-Pradalier G, Diamond P H, Grandgirard V, Sarazin Y, Abiteboul J, Garbet X, Ghendrih Ph, Strugarek A, Ku S and Chang C S 2010 *Phys. Rev. E* **82** 025401(R)
- [40] Jolliet S and Idomura Y 2012 *Nucl. Fusion* **52** 023026
- [41] Gürçan Ö D, Vermare L, Hennequin P, Berionni V, Diamond P H, Dif-Pradalier G, Garbet X, Ghendrih P, Grandgirard V, McDevitt C J, Morel P, Sarazin Y, Storelli A, Bourdelle C and the Tore Supra Team 2013 *Nucl. Fusion* **53** 073029
- [42] Bernstein I B, Greene J M and Kruskal M D 1957 *Phys. Rev.* **108** 546
- [43] Berk H L, Nielson C W and Roberts K W 1970 *Phys. Fluids* **13** 980
- [44] Dupree T H 1970 *Phys. Rev. Lett.* **25** 789
- [45] Dupree T H 1972 *Phys. Fluids* **15** 334
- [46] Dupree T H 1982 *Phys. Fluids* **25** 277
- [47] Berman R H, Tetreault D J and Dupree T H 1983 *Phys. Fluids* **26** 2437
- [48] Tetreault D J 1983 *Phys. Fluids* **26** 3247
- [49] Wang X, Briguglio S, Chen L, Di Troia C, Fogaccia G, Vlad G and Zonca F 2012 *Phys. Rev. E* **86** 045401(R)
- [50] Vlad G, Briguglio S, Fogaccia G, Zonca F, Fusco V and Wang X 2013 *Nucl. Fusion* **53** 083008
- [51] Chen L and Zonca F 2014 *JPS Conf. Proc.* **1** 011001
- [52] Zonca F and Chen L 2014 *AIP Conf. Proc.* **1580** 5
- [53] Briguglio S, Wang X, Zonca F, Vlad G, Fogaccia G, Di Troia C and Fusco V 2014 *Phys. Plasmas* **21** 112301
- [54] Meerson B and Friedland L 1990 *Phys. Rev. A* **41** 5233
- [55] Fajans J and Friedland L 2001 *Am. J. Phys.* **69** 1096

- [56] Chen L 1994 *Phys. Plasmas* **1** 1519
- [57] Briguglio S, Vlad G, Zonca F and Kar C 1995 *Phys. Plasmas* **2** 3711
- [58] Wang X, Briguglio S, Chen L, Di Troia C, Fogaccia G, Vlad G and Zonca F 2011 *Phys. Plasmas* **18** 052504
- [59] Frieman E A and Chen L 1982 *Phys. Fluids* **25** 502
- [60] Brizard A J and Hahm T S 2007 *Rev. Mod. Phys.* **79** 421
- [61] Dicke R H 1954 *Phys. Rev.* **93** 99
- [62] Bonifacio R, De Salvo L, Pierini P and Piovella N 1990 *Nucl. Instrum. Methods Phys. Res., Sect. A* **296** 358
- [63] Zonca F and Chen L 2014 *Phys. Plasmas* **21** 072120
- [64] Zonca F and Chen L 2014 *Phys. Plasmas* **21** 072121
- [65] Chen L, Lin Z and White R B 2000 *Phys. Plasmas* **7** 3129
- [66] Chen L, Lin Z, White R B and Zonca F 2001 *Nucl. Fusion* **41** 747
- [67] Chen L, White R B and Zonca F 2004 *Phys. Rev. Lett.* **92** 075004
- [68] Zonca F, White R B and Chen L 2004 *Phys. Plasmas* **11** 2488
- [69] Chirikov B V 1979 *Phys. Rep.* **52** 263
- [70] Lichtenberg A J and Lieberman M A 1983 *Regular and Stochastic Motion* (Springer - Verlag)
- [71] Berk H L and Breizman B N 1990 *Phys. Fluids B* **2** 2246
- [72] Breizman B N and Sharapov S E 2011 *Plasma Phys. Control. Fusion* **53** 054001
- [73] Briguglio S, Zonca F and Vlad G 1998 *Phys. Plasmas* **5** 3287
- [74] Zhang H S, Lin Z and Holod I 2012 *Phys. Rev. Lett.* **109** 025001
- [75] Chen L and Zonca F 1995 *Phys. Scr.* **T60** 81
- [76] Zonca F and Chen L 1996 *Phys. Plasmas* **3** 323
- [77] Wang Z, Lin Z, Holod I, Heidbrink W W, Tobias B, Van Zeeland M and Austin M E 2013 *Phys. Rev. Lett.* **111** 145003
- [78] Chen L and Zonca F 2013 *Phys. Plasmas* **20** 055402
- [79] Berk H L and Breizman B N 1990 *Phys. Fluids B* **2** 2226
- [80] Berk H L and Breizman B N 1990 *Phys. Fluids B* **2** 2235
- [81] Berk H L, Breizman B N and Pekker M 1996 *Phys. Rev. Lett.* **76** 1256
- [82] Berk H L, Breizman B N and Petiashvili N V 1997 *Phys. Lett. A* **234** 213
- [83] Breizman B N, Berk H L, Pekker M, Porcelli F, Stupakov G V and Wong K L 1997 *Phys. Plasmas* **4** 1559
- [84] Berk H L, Breizman B N, Candy J, Pekker M and Petiashvili N V 1999 *Phys. Plasmas* **6** 3102
- [85] Ge Wang and Berk H L 2012 *Nucl. Fusion* **52** 094003
- [86] Ge Wang 2013 *Ph. D. Thesis* (Austin, TX: University of Texas)
- [87] Breizman B N 2011 *Fus. Sci. Technol.* **59** 549
- [88] Mynick H E and Pomphrey N 1994 *Nucl. Fusion* **34** 1277
- [89] Friedland L, Khain P and Shagalov A G 2006 *Phys. Rev. Lett.* **96** 225001
- [90] Deng W, Lin Z, Holod I, Wang X, Xiao Y and Zhang W 2010 *Phys. Plasmas* **17** 112504
- [91] Deng W, Lin Z, Holod I, Wang Z, Xiao Y and Zhang H 2012 *Nucl. Fusion* **52** 043006
- [92] Tobias B J, Classen I G J, Domier C W, Heidbrink W W, Luhmann Jr N C, Nazikian R, Park H K, Spong D A and Van Zeeland M A 2011 *Phys. Rev. Lett.* **106** 075003
- [93] Zonca F and Chen L 2000 *Phys. Plasmas* **7** 4600
- [94] Briguglio S, Vlad G, Zonca F and Fogaccia G 2002 *Phys. Lett. A* **302** 308
- [95] Zonca F, Briguglio S, Chen L, Dettrick S, Fogaccia G, Testa D and Vlad G 2002 *Phys. Plasmas* **9** 4939
- [96] Vlad G, Briguglio S, Fogaccia G and Zonca F 2004 *Plasma Phys. Control. Fusion* **46** S81
- [97] Briguglio S, Fogaccia G, Vlad G, Zonca F, Shinohara K, Ishikawa M and Takechi M 2007 *Phys. Plasmas* **14** 055904
- [98] Park W, Parker S, Biglari H, Chance M, Chen L, Cheng C Z, Hahm T S, Lee W W, Kulsrud R, Monticello D, Sugiyama L and White R B 1992 *Phys. Fluids B* **4** 2033

- [99] White R B 2012 *Commun. Nonlinear Sci. Numer. Simul.* **17** 2200
- [100] Vlad G, Zonca F and Briguglio S 1999 *Riv. Nuovo Cimento* **22** 1
- [101] Vlad G, Briguglio S, Fogaccia G, Zonca F and Schneider M 2006 *Nucl. Fusion* **46** 1
- [102] Vlad G, Briguglio S, Fogaccia G, Zonca F, Di Troia C, Heidbrink W W, Van Zeeland M A, Bierwage A and Wang X 2009 *Nucl. Fusion* **49** 075024
- [103] Bierwage A, Todo Y, Aiba N, Shinohara K, Ishikawa M and Yagi M 2011 *Plasma Fus. Res.* **6** 2403109
- [104] Bierwage A, Aiba N, Todo Y, Deng W, Ishikawa M, Matsunaga G, Shinohara K and Yagi M 2012 *Plasma Fus. Res.* **7** 2403081
- [105] Qiu Z, Chen L and Zonca F 2014 *Proceedings of the 41.st EPS Conference on Plasma Physics, Berlin, Germany, 23 - 27 June, (2014)*, ECA vol 38F (EPS) Paper No. P4.004
- [106] Chen L, Vaclavik J and Hammett G W 1988 *Nucl. Fusion* **28** 389
- [107] Bergkvist T and Hellsten T 2004 *Theory of Fusion Plasmas* ed Connor J W, Sauter O and Sindoni E (Bologna, Italy: Editrice Compositori, Società Italiana di Fisica) p 123
- [108] Bergkvist T, Hellsten T, Johnson T and Laxåback M 2005 *Nucl. Fusion* **45** 485
- [109] Fu G Y, Lang J, Chen Y, Berk H L, Fredrickson E, Gorelenkov N and Podestà M 2010 *Proceedings of the 23rd International Conference on Fusion Energy 2010* (Vienna: International Atomic Energy Agency) CD-ROM file THW/2-2Rb
- [110] Lang J and Fu G Y 2011 *Phys. Plasmas* **18** 055902
- [111] Lu Z X, Zonca F and Cardinali A 2012 *Phys. Plasmas* **19** 042104
- [112] Dewar R L, Manickam J, Grimm R C and Chance M S 1981 *Nucl. Fusion* **21** 493
- [113] Dewar R L, Manickam J, Grimm R C and Chance M S 1982 *Nucl. Fusion* **22** 307
- [114] Guo Z, Chen L and Zonca F 2009 *Phys. Rev. Lett.* **103** 055002
- [115] Chen L and Zonca F 2012 *Phys. Rev. Lett.* **109** 145002
- [116] Kosuga Y and Diamond P H 2012 *Phys. Plasmas* **19** 072307
- [117] Zonca F, Briguglio S, Chen L, Fogaccia G and Vlad G 2000 Theoretical Aspects of Collective Mode Excitations by Energetic Ions in Tokamaks *Theory of Fusion Plasmas* ed Connor J W, Sauter O and Sindoni E (Bologna: SIF) p 17
- [118] Zonca F and Chen L 2007 *Proceedings of the 34.th EPS Conference on Plasma Physics, Warsaw, Poland, 2 - 6 July, (2007)*, ECA vol 31F (EPS) CD-ROM file P4.071
- [119] McGuire K, Goldston R and Bell et al M 1983 *Phys. Rev. Lett.* **50** 891
- [120] Kaku M 1993 *Quantum Field Theory: A Modern Introduction* (New York: Oxford University Press, Inc.)
- [121] Drummond W E and Pines D 1962 *Nucl. Fusion Suppl. Pt.* **3** 1049
- [122] Vedenov A A, Velikhov E P and Sagdeev R Z 1961 *Nucl. Fusion* **1** 82
- [123] O'Neil T M 1965 *Phys. Fluids* **8** 2255
- [124] O'Neil T M, Winfrey J H and Malmberg J H 1971 *Phys. Fluids* **14** 1204
- [125] Berk H L, Breizman B N and Pekker M S 1997 *Plasma Phys. Rep.* **23** 778
- [126] Vann R G L, Dendy R O, Rowlands G, Arber T D and d'Ambrumenil N 2003 *Phys. Plasmas* **10** 623
- [127] Vann R G L, Dendy R O and Gryaznevich M P 2005 *Phys. Plasmas* **12** 032501
- [128] Lesur M, Idomura Y and Garbet X 2009 *Phys. Plasmas* **16** 092305
- [129] Lesur M and Idomura Y 2012 *Nucl. Fusion* **52** 094004
- [130] Sagdeev R Z and Galeev A A 1969 *Nonlinear Plasma Theory* (W. A. Benjamin Inc.)
- [131] Connor J W, Hastie R J and Taylor J B 1978 *Phys. Rev. Lett.* **40** 396
- [132] Zonca F and Chen L 1993 *Phys. Fluids B* **5** 3668
- [133] Stix T H 1972 *Plasma Phys.* **14** 367
- [134] Zonca F and Chen L 2013 *Bull. Am. Phys. Soc.* **58**(16) 75
- [135] Gross E P 1961 *Nuovo Cimento* **20** 454
- [136] Pitaevsky L P 1961 *Sov. Phys. JETP* **13** 451
- [137] Zakharov V E 1968 *J. Appl. Mech. Tech. Phys.* **9** 190

- [138] Cary J R and Brizard A J 2009 *Rev. Mod. Phys.* **81** 693
- [139] Boozer A H 1981 *Phys. Fluids* **24** 1999
- [140] Boozer A H 1982 *Phys. Fluids* **25** 520
- [141] White R B 1989 *Theory of Tokamak Plasmas* (Amsterdam: North Holland)
- [142] Lichtenberg A J and Lieberman M A 2010 *Regular and Chaotic Dynamics* 2nd ed (Springer - Verlag)
- [143] Levin M B, Lyubarskii M G, Onishchenko I N, Shapiro V D and Shevchenko V I 1972 *Zh. Eksp. Teor. Fiz.* **62** 1725
- [144] Levin M B, Lyubarskii M G, Onishchenko I N, Shapiro V D and Shevchenko V I 1972 *Sov. Phys. JETP* **35** 898
- [145] Wu Y, White R B, Chen Y and Rosenbluth M N 1995 *Phys. Plasmas* **2** 4555
- [146] Xiao Y and Lin Z 2011 *Phys. Plasmas* **18** 110703
- [147] Gustafson K, Ricci P, Furno I and Fasoli A 2012 *Phys. Rev. Lett.* **108** 035006
- [148] Gustafson K, Ricci P, Bovet A, Furno I and Fasoli A 2012 *Phys. Plasmas* **19** 062306
- [149] Feng Z, Qiu Z and Sheng Z 2013 *Phys. Plasmas* **20** 122309
- [150] Fredrickson E D, Crocker N A, Bell R E, Darrow D S, Gorelenkov N N, Kramer G J, Kubota S, Levinton F M, Liu S, Medley S S, Podestà M, Tritz K, White R B and Yuh H 2009 *Phys. Plasmas* **16** 122505
- [151] Podestà M, Bell R E, Crocker N A, Fredrickson E D, Gorelenkov N N, Heidbrink W W, Kubota S, LeBlanc B P and Yuh H 2011 *Nucl. Fusion* **51** 063035
- [152] Podestà M, Bell R E, Bortolon A, Crocker N A, Darrow D S, Diallo A, Fredrickson E D, Fu G-Y, Gorelenkov N N, Heidbrink W W, Kramer G J, Kubota S, LeBlanc B P, Medley S S and Yuh H 2012 *Nucl. Fusion* **52** 094001
- [153] Zonca F and Chen L 2000 Destabilization of Energetic Particle Modes by ICRF induced fast minority ion tails on TFTR *Proceedings of the 6.th IAEA TCM on Energetic Particles in Magnetic Confinement Systems* (Naka, Japan: JAERI-Conf 2000-004) p 52
- [154] Fu G Y, Park W, Strauss H R, Breslau J, Chen J, Jardin S and Sugiyama L E 2006 *Phys. Plasmas* **13** 052517
- [155] Vlad G, Briguglio S, Fogaccia G, Zonca F, Di Troia C, Fusco V and Wang X 2012 Electron Fishbone Simulations in FTU-Like Equilibria Using XHMGC *Proceedings of the 24th International Conference on Fusion Energy* (Vienna: International Atomic Energy Agency) CD-ROM file TH/P6-03 and <http://www-naweb.iaea.org/naweb/physics/FEC/FEC2012/papers/77-THP603.pdf>